ADVANCED NANOBIOMED RESEARCH Open Access
www.advnanobiomedres.com

Recent Technological Developments in the Diagnosis and Treatment of Cerebral Edema

Karthikeya P. Deshmukh, Sajjad Rahmani Dabbagh, Nan Jiang, Savas Tasoglu, and Ali K. Yetisen**

Latest technological advancements in neurocritical care have translated to improved clinical outcomes and have paved the way for the effective diagnosis and treatment of cerebral edema. Effective management of cerebral edema has the potential to provide a personalized treatment by obtaining the complete pathophysiological information of the patient. The aims of this review are to inform the reader about the research and development in this field in the past decade as well as the materialization of scientific literature through patents. There is a growing interest in multimodal monitoring of the diseased brain as it provides a necessary means to implement effective intervention strategies. Although there is a gradual shift toward the adoption of noninvasive devices for research purposes, their clinical applications are hindered by their inaccuracies. However, the inherent risk of complication and high costs of implementation challenge the status quo. The role of neuroprotectants is explored and the combination of neurodiagnostic and neuroprotective approaches is proposed. Finally, the impacts of the current state of global affairs are discussed and it is predicted that the rising number of traumatic brain injury patents will inevitably translate to improvements in technologies to effectively address cerebral edema.

1. Introduction to Neurocritical Care

Neurocritical care aims to provide brain-specific care to improve the outcomes of critically ill spine- and brain-injured patients.[1] These conditions may have arisen due to a multitude of reasons, including acquired brain injury (ABI) such as ischemic stroke, hemorrhage, and traumatic brain injury (TBI).[2] Globally, more than 50 million individuals suffer from TBI each year and it is the major source of disability and morbidity. Around 3.17 million TBI patients experience posttraumatic complications ranging from neurological and psychosocial problems to long-term disability.[3] On a global scale, the expenditure is typically more than $200 billion.[4] In the United States, around 1.7 million people suffer a traumatic brain injury each year. Of these, ≈52 000 people die and 80 000 experience a debilitating form of disability.[5] This population is twice as likely to die in 3.5 years following TBI compared to the general population.[4] The treatment, hospitalization, and rehabilitation after a traumatic brain injury cost the US economy $48.3 billion annually. Although this underscores the tremendous economic impact of TBI, its social impacts are often overlooked. These include cognitive impairment, and disturbances in memory, attention, behavior, and emotion, which can translate to poor quality of life. Therefore, the management of the aftermath of TBI is equally important.[6]

According to Busl et al.,[7] neurointensive care units (neuroICUs) are seen to positively affect the financial state of healthcare systems. The length of stay decreased by 25–45% below the benchmark for a similar ICU admission, thus offering significant cost savings of over $5900 per average case.[7] Continual developments in neurocritical care have underpinned multidisciplinary research in neuromonitoring and neurocritical care information technology to become an integral part of healthcare systems in tackling ABI globally.

Neurological disease diagnosis and prognosis can be facilitated by a multitude of monitoring techniques, some of which have been commercialized successfully, while the others are en route to being commercialized in the form of patents. This review aims to educate the reader on the current diagnostic tool available on the market, the cutting-edge technology in the

K. P. Deshmukh, A. K. Yetisen
Department of Chemical Engineering
Imperial College London
Imperial College Road, Kensington, London SW7 2AZ, UK
E-mail: a.yetisen@imperial.ac.uk

S. Rahmani Dabbagh, S. Tasoglu
Department of Mechanical Engineering
Koc University
Rumelifeneri Yolu, Sariyer, Istanbul 34450, Turkey
E-mail: stasoglu@ku.edu.tr

N. Jiang
West China School of Basic Medical Sciences & Forensic Medicine
Sichuan University
Chengdu 610041, China

S. Tasoglu
Boğaziçi Institute of Biomedical Engineering
Boğaziçi University
Istanbul 34684, Turkey

The ORCID identification number(s) for the author(s) of this article can be found under https://doi.org/10.1002/anbr.202100001.

© 2021 The Authors. Advanced NanoBiomed Research published by Wiley-VCH GmbH. This is an open access article under the terms of the Creative Commons Attribution License, which permits use, distribution and reproduction in any medium, provided the original work is properly cited.

DOI: 10.1002/anbr.202100001

26999307, 2021, 11, Downloaded from https://advanced.onlinelibrary.wiley.com/doi/10.1002/anbr.202100001 by Koc University, Wiley Online Library on [05/09/2026]. See the Terms and Conditions (https://onlinelibrary.wiley.com/terms-and-conditions) on Wiley Online Library for rules of use; OA articles are governed by the applicable Creative Commons License

form of patents, and offer a preview of the technologies in the research phase that are set to dominate the scene of future neurodiagnostic technology.

1.1. The Need for Cerebral Edema Monitoring

Cerebral edema occurs as a swelling caused by excess accumulation of fluids in the intracellular and extracellular space of the brain tissue.[8] It is a common neurological disease and often occurs as a complication of TBI and nontraumatic brain injuries (NTBIs) such as intracerebral hemorrhage or cerebral infarction.[9] The impact of fluid build-up is an increase in intracranial pressure. This restricts blood flow and leads to ischemic and hypoxic insults.[10,11] If not intervened, this can lead to severe neurologic damage such as herniation. Hence, early identification of edema can mitigate the subsequent increase in intracranial pressure (ICP) and prevent irreparable damage.

Cerebral edema is dichotomized into cytotoxic and vasogenic types[12]; the following sections explore these in greater detail. The real-time and continuous monitoring of cerebral edema can help to target therapy rapidly and accurately. It can be an early indicator for ischemia and provide information on edema prognosis.[9,13] The information accrued can be used to devise personalized therapies with real-time monitoring capabilities to gauge the impact of the treatments imparted through a multitude of modalities. Ultimately, it may help elucidate the neuropathophysiology of patients who undergo brain-related injuries to minimize fatalities caused by cerebral edema.[6]

2. Cerebral Pathophysiology of Acquired Brain Injury

ABI, a rapidly growing public health concern, has led to nearly 1000 hospital admissions each day in the United Kingdom, and has followed a 10% increase from the previous decade.[14] ABI can be broadly categorized into two types, namely, traumatic brain injury and nontraumatic brain injury. The following sections elaborate on these.

2.1. TBI

TBI is the prime cause of functional disruption caused due to the application of blunt or penetrating trauma, such as those caused by motor vehicle crashes, suicides, falls, and assault.[15] TBI can be categorized into primary and secondary injuries. Primary brain injury is a consequence of direct impact to the brain parenchyma. It can be either diffuse or focal depending on the physics of the impact and manifests itself as contusion, axonal shearing, and blood vessel impairment.[16,17] Due to the nature of the injury, the primary injury cannot be treated, but the delay in the onset of secondary injury can be intervened through therapeutic means.[18]

The secondary brain injury results as pathophysiological and biochemical disruptions brought about by a combined effect of neuronal and glial dysfunction, metabolic and inflammatory processes triggered by the release of various signaling and inflammatory molecules from neuronal, glial, and immune cells.[16,17] The delay between the primary and secondary injuries may be exploited for an effective administration of treatments.[6]

There are several means of clinical assessments and prognosis in patients with TBI. Among these, the Glasgow Coma Scale (GCS), which was developed in 1974, is the most widely used.[19] It consists of three components—eye-opening, verbal, and motor response—and these are used to determine a person's level of consciousness. However, TBI severity can be misclassified because external factors such as medical sedation and drug intoxication can interfere with the consciousness of the patient.[18] Hence, to obtain a better estimate of the TBI severity, a holistic approach is taken that encompasses imaging modalities such as computed tomography (CT) to assess structural damage as well as the Abbreviated Injury Scale (AIS), which ranks the extent of injury from minor (1) to nonsurvivable (6). **Table 1** stipulates the criteria used to classify TBI severity and provides the mortality rate for each of the three intensities of TBI: mild, moderate, and severe.

2.2. NTBI

NTBI accounts for the nonimpact injuries, which can result from infections, oxygen deprivation due to high altitude, metabolic disorders, and heavy metal poisoning, to name but a few.[20,21] Despite improvements in emergency care and consequential increase in survival rates through stroke units, trauma centers, and bystander cardiopulmonary resuscitation, the provision of neurorehabilitation for survivors is limited. Poor understanding of the consequences of NTBI hinders the reintegration of NTBI patients into society and underscores the importance of research in this area.[14]

Treatment of NTBI is aimed at preventing or minimizing the damage caused by secondary injury.[22] Thus, monitoring the brain tissue biochemistry allows the identification of impending secondary injury and allows the timely implementation of neuroprotective strategies, which are discussed in greater detail in this review. Cerebrospinal fluid (CSF) contains numerous inflammatory biomarkers and their identification allows the analysis of the underlying disease mechanisms to devise a therapeutic response to the underlying conditions.[23] **Table 2** gives a breakdown of the conditions, briefly describes the condition, and reports the biomarkers of interest.

Although TBI is the prime cause of cerebral edema, other cases of NTBI such as hyponatremia (liver failure), cardiac arrest,

Table 1. Prognostic tools for the assessment of TBI.

Criteria[a)]	Mild	Moderate	Severe
Structural imaging (CT)	Normal	Normal or abnormal	Normal or abnormal
Loss of consciousness	<30 min	30 min–24 h	>24 h
Posttraumatic amnesia [days]	0–1	>1 and <7	>7
GCS	13–15	9–12	3–8
AIS: Head	1–2	3	4–6
Mortality rate	1.6%	10.1%	84.7%

[a)]Data obtained from ref. [101] and ref. [19].

© 2021 The Authors. Advanced NanoBiomed Research published by Wiley-VCH GmbH

26999307, 2021, 11, Downloaded from https://advanced.onlinelibrary.wiley.com/doi/10.1002/anbr.202100001 by Koc University, Wiley Online Library on [05/09/2026]. See the Terms and Conditions (https://onlinelibrary.wiley.com/terms-and-conditions) on Wiley Online Library for rules of use; OA articles are governed by the applicable Creative Commons License

Table 2. Different types of brain conditions arising from TBI and NTBI and the key biomarkers in CSF.

Condition	Description	Key biomarker in CSF	Reference
Multiple sclerosis	Autoimmune disease where nerves are targeted	Immunoglobulin G, A, and M, glucose (CSF to serum ratio), lactate, albumin CSF+/serum ratio	[23]
Myelitis	Inflammation of the spinal cord	14-3-3 Theta/tau protein, cystatin C	[102]
Encephalitis	Inflammation of the brain cells	8-Hydroxy-2′-deoxyguanosine (8-OHdG), hexanoyl-lysine adduct (HEL), tau protein and cytokines	[103]
Meningitis	Inflammation of the meninges due to infection	C-reactive protein (CRP), α1-antitrypsin (AAT), α1-acid glycoprotein (AAG), haptoglobin (HPT), ceruloplasmin (CER)	[104]
Edema	Inflammation caused due to fluid retention	Interleukin-8 (IL-8), tumor necrosis factor (TNF-α), aquaporin-4 (AQP4)	[105]
Leukemia	Blood cancer	Total-tau (T-tau), CSF glial fibrillary acidic protein (GFAP), calcium-binding protein β (S100β)	[106,107]
Dementia	Neurocognitive disorder caused by Alzheimer's	Amyloid β (Aβ)-42, T-tau, phosphorylated-tau (P-tau) for Alzheimer's disease	[108]

and stroke may also initiate the development of cerebral edema. It may also stem from other chronic brain conditions such as brain tumors, cerebral ischemia, infarction, contusion, and hypertensive encephalopathy.[1,6,24,25] Cerebral edema also occurs as a complication to epilepsy surgery and other invasive procedures.[26] However, this review aims to explore the traumatic origins of cerebral edema.

3. Mechanisms of Cerebral Edema Development

Latest advances in cerebral edema research have revealed numerous pathophysiologic pathways that contribute to their development. These include the disruption of blood–brain barrier (BBB) integrity, dysfunction in ionic pumps that regulate the cellular volume, presence of oncotic gradients, and responses to inflammation.[13] The following subsections elaborate on the underlying mechanisms and **Figure 1**a shows the complex interplay between these mechanisms.

3.1. Primary Injury Mechanism

Primary injuries occur due to stretching of the cellular membranes of the neurons and cause unregulated neuronal immigration of sodium (Na^+) ions, the emigration of potassium (K^+) ions, and increase in intraaxonal Ca^{2+} ions.[4,27] The high osmolarity in the necrotic core of the contusion creates a water flux and causes acute swelling of the contusion.[13] Primary injury inevitably leads to secondary injury in moderate and severe cases as the abundance of Ca^{2+} activates protease and calpain and triggers the calpain-mediated proteolysis of cytoskeletal proteins. This inevitably causes an irreversible pathology in axons.[28] The continual attempt of membrane pumps to restore ionic homeostasis depletes glucose, which causes an influx of Ca^{2+} into mitochondria and produces lactate, which initiates acidosis and edema.[4,28] Neurosurgeons have limited power in repairing the damage caused by the primary injury; it is imperative to treat the secondary injuries as these hold the potential to cause severe and prolonged brain damage.[29]

3.2. Secondary Injury and Disruption of the BBB

Secondary injury, which follows on from primary injury, can be more devastating and can last for 5–10 days. These account for 80% of the severe injury deaths; hence, it is important to timely address the secondary injuries.[6] Secondary injury can cause physiological perturbations which disrupt the body's homeostatic equilibrium. This can occur by initiating an inflammatory response that increases the concentration of free radicals at the site of contusion. The BBB is rendered hyperpermeable and inevitably leads to cerebral edema that is vasogenic in origin.[5] Plasma-derived factors and immune cells extravasate into the extracellular space, which causes an increase in the total brain volume.[4] The elevation in extracellular oncotic pressure exacerbates this process and causes a surge in intracranial pressure, changes in cerebral blood flow, tissue swelling, and cerebral herniation.[4] The caveat in these mechanisms is the interrelation of all the biomolecular pathways, so each of the processes cannot be uniquely defined.[13]

3.3. Classification and Mechanisms of Cerebral Edema

The underlying mechanisms of cerebral edema formation may be influenced by a multitude of different factors, including the nature of the primary injury (such as etiology and severity), patient characteristics (such as age and gender), as well as additional insults (such as hypoxia).[13] Although active research in this area has uncovered several mechanisms for the development of cerebral edema, our understanding of the complex biomolecular pathways is just the tip of the iceberg.[13] Despite the dichotomization of edema vasogenic and cytotoxic forms, they are inextricably interlinked.[12,13] Many other types of cerebral edemas have been identified, and these are reported in **Table 3**.

Cytotoxic edema is a consequence of the ionic pump failure, activation, and upregulation of various ion channels (including AQP4, ASIC, NHE, NBC, AVP, NKCC1, NMDA-R, EAAT1/2, and Surf-Trpm4). This declines the homeostatic equilibrium of the ionic gradients and allows the flow of water from the

 © 2021 The Authors. Advanced NanoBiomed Research published by Wiley-VCH GmbH

interstitial to intracellular space in the form of edema.[30] Cytotoxic edema has been reported as early as 1 h post-TBI in humans and in all cell types including neural, astroglial, and endothelial cells, where excessive water accumulation is known to cause blebbing and oncotic cell death within 1–7 days.[31] Although this mechanism does not change the total brain water content, the complex interplay between the osmotically driven perfusion from the cerebral vasculature and the enhanced CSF influx or impaired efflux of the glymphatic system is implicated for the burgeoning water content.[13,31] Figure 1b provides a visual representation of the cytotoxic edema development mechanism.

When the aforementioned process occurs in endothelial and astroglial cells constituting the BBB, it contributes to vasogenic edema. Several etiologies contribute to vasogenic edema formation, including mechanical disruption and disease cascades, including proinflammatory cytokines/neuroinflammation.[13,32] The release of proinflammatory cytokines and chemokines

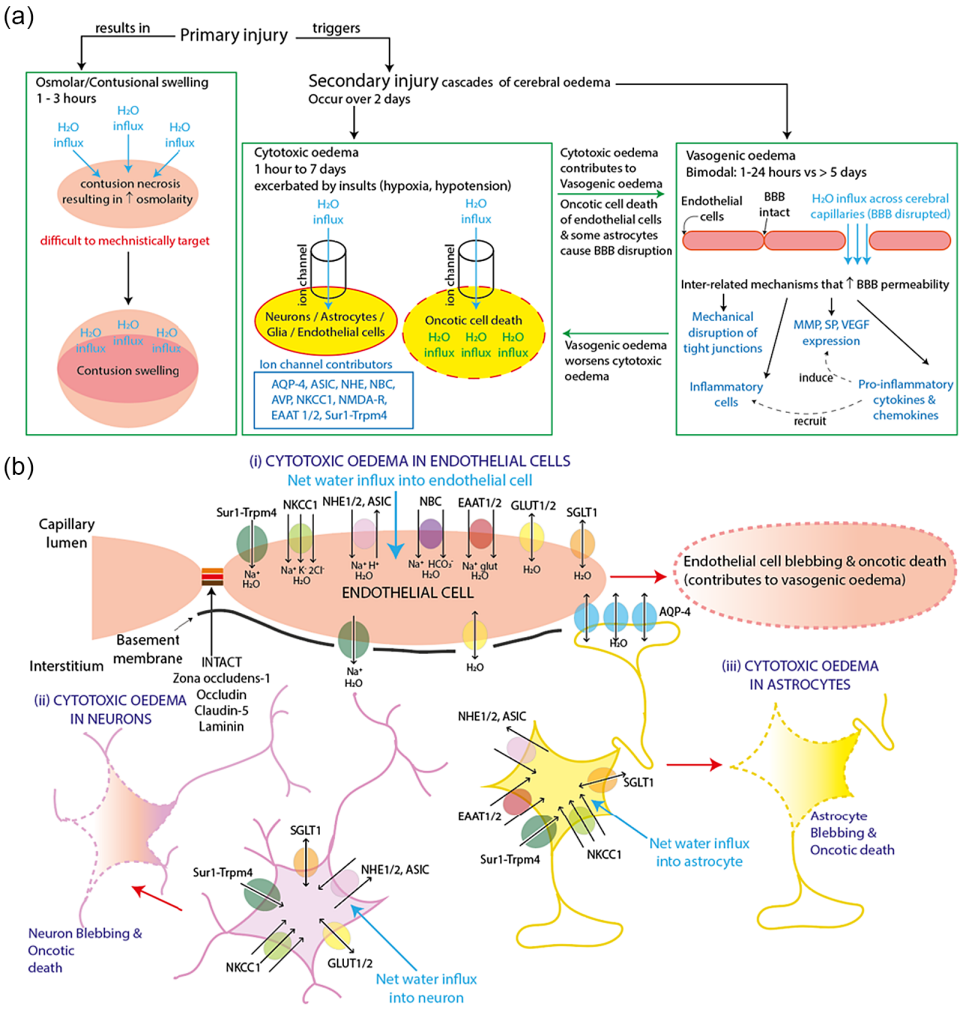


Figure 1. Mechanisms of cerebral edema development through primary and secondary mechanisms. a) Mechanisms of primary injury, which results in osmolar or contusional swelling, and secondary injury, which causes cytotoxic and vasogenic edema. b) Mechanisms leading to cytotoxic edema development. (i) Net water influx that is driven by ionic contributors such as GLUT1/2, Sur1-Trpm4, NKCC1, NHE1/2, ASIC, NBC, EAAT1/2, and SGLT1 that cause the endothelial cell to swell. These cotransport water with ions. The tight junctions (solid orange, brown, and red linkages between endothelial cells) and the basement membrane (solid gray line under the endothelial cells) are intact. (ii) Cellular swelling in neurons and (iii) astrocytes or astroglial cells caused by Na^+ and water entering the cells by the same mechanism described previously, which eventually causes cell blebbing and oncotic cell death, as shown by dashed lines. Astrocytic endfeet (lasso-like loops) express aquaporin-4 (AQP-4) at the blood–brain and blood–CSF junctions, which enable passive water by osmotic pressure or pressure gradient. c) Mechanisms contributing to vasogenic edema following TBI. (i) Edema formation triggered by cellular retraction in myosin light chain kinase contraction of the cytoskeleton as well as cytotoxic edema in endothelial cells which leads to disruption and cellular oncotic death. (ii) Contribution of decreased water efflux to vasogenic edema by a loss of polarization of AQP-4 in the perivascular and perependymal endfeet. Endfeet of astrocytes undergoing blebbing and oncotic death cannot seal the BBB, which exacerbates vasogenic edema. (iii) Downregulation of tight junction proteins zona occludens-1, occludin, claudin-5 and disruption of the basement membrane. (iv) Activation and migration of inflammatory cells worsens vasogenic edema. PMN adhere to the endothelial cells via upregulated receptors or ligands such as VCAM-1, VLA4, ICAM-1, and LFA-1. Chemokines assist their migration into the interstitial space. Adapted with permission.[13] Copyright 2019, Elsevier Ltd. Single-headed arrows represent water cotransport, whereas double-headed arrows represent passive water transport through a channel pore.

© 2021 The Authors. Advanced NanoBiomed Research published by Wiley-VCH GmbH

26999307, 2021, 11, Downloaded from https://advanced.onlinelibrary.wiley.com/doi/10.1002/anbr.202100001 by Koc University, Wiley Online Library on [05/09/2026]. See the Terms and Conditions (https://onlinelibrary.wiley.com/terms-and-conditions) on Wiley Online Library for rules of use; OA articles are governed by the applicable Creative Commons License

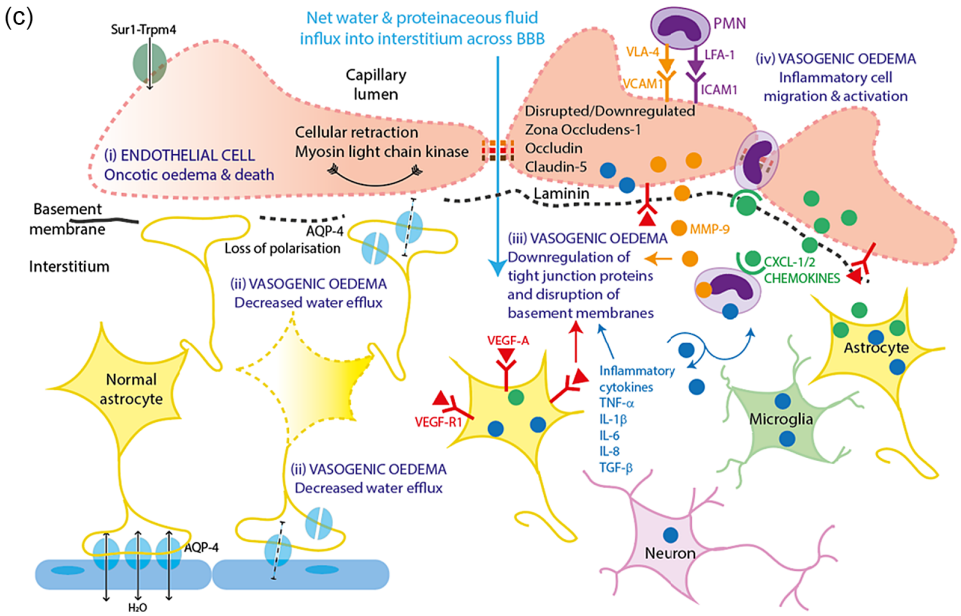


Figure 1. Continued.

Table 3. Classification of cerebral edema into seven types.

Edema type[a)]	Location	Site	BBB integrity	Postulated mechanism and manifestation	Disease	Mitigation of damage
Vasogenic edema	Extracellular	White matter	Disrupted	Increased vascular permeability to plasma components Leakage in capillaries Build-up of water in interstitial space	Tumor Trauma Meningitis Abscess ICH	Reversible in principle
Cytotoxic edema	Intracellular	White and gray	Intact	Energy failure (Na^+/K^+ pump failure) Loss of ionic gradients Water transport from extra to intracellular space	Anoxia Overhydration Toxins Hydrocephalus Reye's syndrome	Irreversible
Ischemic edema	Intracellular and extracellular	White and gray	Disrupted	Anoxia	Cerebral ischemia Intracerebral hemorrhage	NR
Hydrostatic edema	Extracellular	White and grey	Disrupted	Increased blood pressure	Hypertensive encephalopathy	NR
Hydrocephalic edema	Extracellular	White	Intact	Periventricular extravasation	Hydrocephalus Pseudotumor cerebri	NR
Osmotic edema	Intracellular and extracellular	White and gray	Intact	Plasma hypoosmolality	Overhydration SIADH Malignant hypertension	NR
Interstitial edema	Extracellular	White	Intact	CSF leak Hydrostatic pressure elevation	Hydrocephalus	NR

[a)]Adapted from Refs.[30,109,119,120]; NR indicates not reported; SIADH = syndrome of inappropriate antidiuretic hormone secretion; ICH = intracerebral hemorrhage.

increases the expression and release of factors such as matrix metalloproteinase (MMP), substance P (SP), and vascular endothelial growth factor (VEGF) that disrupt tight junctions and basement membrane proteins. The proteinaceous fluid influx may further raise oncotic pressure in the interstitium, which occludes small vessels and causes local hypoperfusion, which may aggravate cytotoxic edema and upregulation of ion channels such as sulfonyl receptor 1–transient receptor potential cation

© 2021 The Authors. Advanced NanoBiomed Research published by Wiley-VCH GmbH

26999307, 2021, 11, Downloaded from https://advanced.onlinelibrary.wiley.com/doi/10.1002/anbr.202100001 by Koc University, Wiley Online Library on [05/09/2026]. See the Terms and Conditions (https://onlinelibrary.wiley.com/terms-and-conditions) on Wiley Online Library for rules of use; OA articles are governed by the applicable Creative Commons License

channel subfamily M member 4 (Sur1-Trpm4). BBB has the greatest permeability that has been reported within the first few hours postinjury and can persist for 3–4 days; another peak is noted after 5 days, which is mediated by microglial activation.[32,33] Figure 1c shows the vasogenic edema development mechanism.

Further classification of cerebral edema has been made to account for the latest discoveries in the mechanisms of edema development. Table 3 provides a succinct summary of all seven types of cerebral edema identified along with their postulated mechanisms of development to guide the interested reader.

4. Establishing the Need for Neuromonitoring of Cerebral Edema

Neuromonitoring plays a pivotal role in guiding therapeutic interventions intended to prevent or minimize secondary injury.[34] Recent developments in these novel techniques have greatly improved the utility and accuracy of neurophysiological monitoring, and have now become an integral part of mainstream surgical procedures.[35] These techniques are also useful in assessing the response of the injured brain to treatment.[34] The overarching goal is the detection and reversal of secondary injury.

4.1. Multimodality of Neuromonitoring

Multimodal monitoring is the simultaneous measurement of several parameters of brain function, which may provide vital information about the underlying pathophysiology by medical or surgical intervention.[36] This is imperative due to the absence of a single neuromonitor that is capable of measuring a thorough spectrum of pathophysiologic changes after TBI.[34] Multimodal monitoring offers a promising tool to tailor treatments for seemingly similar pathological conditions by enabling distinctions between them. However, there is uncertainty surrounding the most clinically relevant physiological variables, the most appropriate methods of monitoring them, and the most financially viable options.[34]

A consensus of experts in multimodal neuromonitoring emphasizes the effectiveness of invasive techniques in acquiring accurate data.[37] Additionally, they stress the need for the development of point-of-care neuromonitoring techniques despite the absence of high-quality data; this factors in the advancements in technologies that will lead to a culture of high-functionality, noninvasive, and real-time devices with significant ease of operation and miniaturization.[37]

4.2. Invasive and Noninvasive Neuromonitoring

Invasive methods are seen to be the most accurate means of measuring cerebral parameters such as ICP and cerebral metabolism. The main types of invasive techniques include ventriculostomy and microtransducers. Ventriculostomy is regarded as the "gold standard" in accurately measuring important cerebral parameters such as ICP.[38] The selection of a device is influenced by the type of injury, the function of the device, and institutional policies, and it may or may not utilize state-of-the-art technology. TBI patients need invasive monitoring for the effective treatment of the underlying conditions.[39] Despite the ubiquity of ICP catheters and their successful implementation, these are highly invasive and increase the risk of complications including infection, hemorrhage, and neurological deficits.[40]

ICP monitoring gives a proxy for monitoring cerebral edema and offers a vital insight into its progression.[41] Ventriculostomy or intraparenchymal catheters are implemented through a burr hole and are secured via a bolt to monitor ICP.[6] However, ICP monitoring encompasses several pathophysiological processes and edema amongst these may be indistinguishable. Despite being a useful modality, ICP, in its own right, does not provide adequate information to understand the underlying pathology.[6] **Figure 2** shows the placement of invasive probes for neuromonitoring and neurosurgery.

Table 4 shows the sites in the brain where these devices are placed for neuromonitoring purposes. It can be noted that the devices near the center of the brain are often very highly accurate compared to those at the periphery.[39] However, the deeply penetrating devices often suffer from a higher risk of infection and other complications. However, those farther from the ventricles can be shown to give reasonable estimates and their results are comparable to noninvasive techniques. These also mitigate the invasiveness and their following complications without a significant decline in the efficacy of results.[34,42]

Noninvasive devices can circumvent the complications and risk of infection; however, they lack the appropriate level of accuracy needed to be able to replace the current economy of invasive devices. Although noninvasive devices allow detection of underlying changes in the brain, no techniques are available to detect fluid changes accurately and continuously as well as obtain an indication of the extent of edema.[41] Noninvasive devices are placed on the scalp and often require the patient to shave their head to minimize interference with the signals and risk of infection.[39,41]

5. Biomarker Analysis Formats and Technologies

Biomarkers are proteins, fragments of proteins, DNA, RNA, or any organic molecules that are synthesized by abnormal cells. These are indicative of a diseased biological state or condition.[43] Hence, these are extremely important for the early detection, progression, and management of diseases through diagnostic interventions.

Traditional techniques for the identification of biomarkers of interest include the enzyme-linked immunosorbent assay (ELISA), radioimmunoassay (RIA), fluorescence immunoassay (FIA), and electrophoretic immunoassay (EPIA). Several specialized assay detection technologies have been established, including Luminex, Gyrolab, Erenna, AlphaLISA, Delfia, Immuno-PCR, and BIAcore.[44] Standard enzyme immunoassays are used to detect antibody, antigen, or a combination thereof. Antibody-detection assays rely on the use of an immobilized antigen that captures any antibody present in the test sample. Conversely, the antigen detection assays are based on the immobilized antibody to capture pathogen-specific antigens.[45]

© 2021 The Authors. Advanced NanoBiomed Research published by Wiley-VCH GmbH

26999307, 2021, 11, Downloaded from https://advanced.onlinelibrary.wiley.com/doi/10.1002/anbr.202100001 by Koc University, Wiley Online Library on [05/09/2026]. See the Terms and Conditions (https://onlinelibrary.wiley.com/terms-and-conditions) on Wiley Online Library for rules of use; OA articles are governed by the applicable Creative Commons License

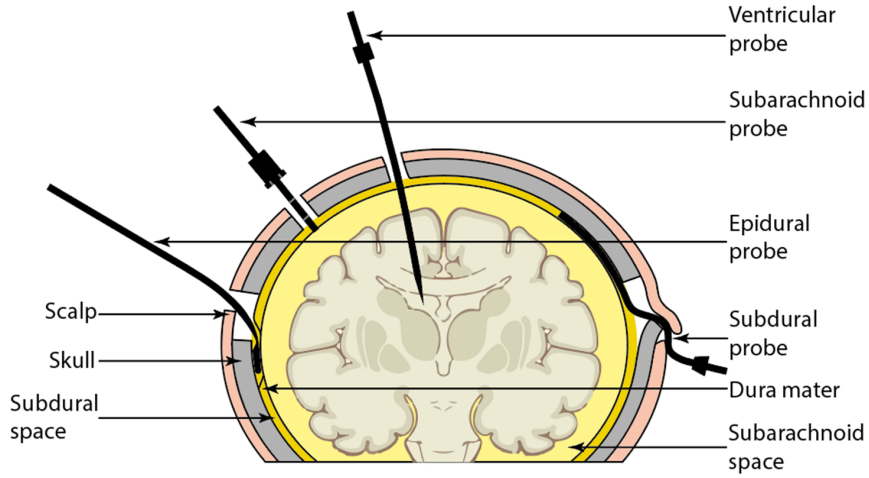


Figure 2. Placement of invasive neuromonitoring and neurosurgical devices into the different regions in the brain. These include ventricles (ventricular probe), subarachnoid space and intraparenchymal space (subarachnoid probe), and subdural space (subdural probe). Adapted with permission.[39] Copyright 2016, Elsevier Inc.

Table 4. Advantages, disadvantages, and placement locations of invasive neuromonitoring device placement sites.

Monitor type[a)]	Location	Advantages	Drawbacks
Ventriculostomy catheter	Ventricles	"Gold standard"	Difficulty in placement
		Measures global ICP	Risk of infection
		Therapeutic drainage of CSF to manage ICP	Risk of hemorrhage
		Reliable and accurate	Possibility of occlusion
		In vivo calibration	Most invasive modality
			Cannot drain CSF and monitor ICP simultaneously
Intraparenchymal monitor	Parenchyma	Ease of placement	In vivo calibration not possible
		Less infectious complications	Fiber optics can be easily damaged
Subdural catheter	Between dura and subarachnoid space	Ease of placement.	Less reliable
		Low complication risk	Poor waveform
		No cerebral penetration	Limited accuracy
			Periodic flushing required
Epidural catheter	Between skull and dura	Ease of placement	Indirect measurement of ICP
		No dural penetration	Less reliable
		Low complication risk	Limited accuracy
			Rarely used

[a)]Adapted from ref. [42], ref. [39], and ref. [34].

The ELISA allows for high-throughput screening and detection of a specific biomarker.[43] It is useful at point of care and can be automated. Disadvantages include being technically burdensome, expensive, long incubation and detection times, and need for additional chemicals.[45,46] Furthermore, traditional diagnostic methods are neither accessible to the general population nor appropriate for repeated screenings at the early stage of disease detection and monitoring.

Traumatic brain injuries inevitably bring about complex biomolecular changes in the brain such as glial activation and secretion of cytokines.[13] Reinstating the biomolecular deviations is shown to improve functional recovery following brain damage caused by traumatic brain injury and other causes.[47] Hence, biomarker analysis technologies provide an alternative means of cerebral edema diagnosis and monitoring.

5.1. Quantitative Discussions on Sensor Performance

The biomarker detection performance of the sensor can be evaluated using the limit of detection (LOD). It represents the lowest analyte concentration that can be detected by the sensor and is expressed mathematically as Equation (1). The limit of quantification (LOQ) represents the lowest concentration at which the analyte concentration can be reliably detected and goals for bias and imprecision can be met and is expressed mathematically as Equation (2).[48] **Table 5** gives the key biomarkers implicated in cerebral edema formation and provides the data on selectivity, sensitivity, LOD, and LOQ (Acquired from Sharma et al.,[49] Acquired from Ben Ismail et al.,[50]).

$$\mathrm{LOD} = \frac{3\sigma}{S} \tag{1}$$

© 2021 The Authors. Advanced NanoBiomed Research published by Wiley-VCH GmbH

26999307, 2021, 11, Downloaded from https://advanced.onlinelibrary.wiley.com/doi/10.1002/anbr.202100001 by Koc University, Wiley Online Library on [05/09/2026]. See the Terms and Conditions (https://onlinelibrary.wiley.com/terms-and-conditions) on Wiley Online Library for rules of use; OA articles are governed by the applicable Creative Commons License

26999307, 2021, 11, Downloaded from https://advanced.onlinelibrary.wiley.com/doi/10.1002/anbr.202100001 by Koc University, Wiley Online Library on [05/09/2026]. See the Terms and Conditions (https://onlinelibrary.wiley.com/terms-and-conditions) on Wiley Online Library for rules of use; OA articles are governed by the applicable Creative Commons License

Table 5. The chemical analytes and detection techniques used for the quantification of selectivity, sensitivity, and LOD, along with other pertinent values.

Analyte[a)]	Detection type[a)]	Probe size	Selectivity/ Sensitivity	Detection range	LOD (LOQ)	Linear range	Reference
Taurine	Electrochemical: graphene quantum dots	NR	High/ 147 565 μA mol^{-1}	NR	0.3* μm [0.001 mM]	NR	[110]
	Enzyme: Fiber optic	600 μm diameter	NR/ 0.0190 AU mM^{-1}	0–1 mM	53 μM [0.177* mM]	NR	[49]
Matrix metalloprotease 9 (MMP-9)	Aptamer-based piezoelectric	42.6 mm^2, 7.4 mm diameter	NR/1.335 Hz nM^{-1} OR 6.8 ± 0.25 pM	0.1–25 nM PBS	1.2 pM (buffer solution) [4* pM] 6.8 pM (untreated serum) [22.7* pM]	NR	[111]
	Calorimetric (ELISA)	NR	NR/3.5 AU mL ng^{-1}	0–0.5 ng mL^{-1}	4–10 pg mL^{-1} [13.3*–33.3* pg mL^{-1}]	30–500 pg mL^{-1}	[50]
	Calorimetric (Magneto ELISA)	NR	NR/2.2 AU mL ng^{-1}	16–1000 pg mL^{-1}	11–30 pg mL^{-1} [36.7*–100* pg mL^{-1}]	16–1000 pg mL^{-1}	[50]
Interleukin-8	Impedimetric immunosensor	2 mm × 20 mm	71%/0.0225* mL fg^{-1}	0–3 pg mL^{-1}	6 fg mL^{-1} [19 fg mL^{-1}]	0.02 pg mL^{-1} to 3 pg mL^{-1}	[46]
	Dual-function microfluidic	NR	high/1 009 000 AU mL pg^{-1}	0–120 pg mL^{-1}	0.252* pM [0.84 pM]	7.5–120 pg mL^{-1} (0.84 pM–13.44 pM)	[112]
Tumor necrosis factor (TNF-α)	ELISA	NR	NR/0.0037 mL pg^{-1}	0–300 pg mL^{-1}	0.48 pg mL^{-1} [1.6* pg mL^{-1}]	0–300 pg mvL	[113]
	Photoluminescence: Quantum-dot-based optical Aptasensor	NR	High/0.8285* nM^{-1}	0–22.5 nM	97.2 pM [324* pM] 1.7 ng/mL [5.67* ng/mL]	0–22.3 nM 1–400 ng/mL	[114]
	Amperometric: Electrochemical immunosensor	NR	NR/9.238* nA mL/ pg	1–1000 pg/mL	0.85 pg/mL [2.83 pg/mL]	1–200 pg mL^{-1}	[115]
Procalcitonin	Quantum dots	NR	NR/0.5659* mA mL ng^{-1}	0.1 μg mL^{-1} to 10 μg mL^{-1}	0.21 ng mL^{-1} [0.7* ng L^{-1}]	N/R	[116]
	Immunosensor: organic field-effect transistor	NR	high/0.14427 M^{-1}	0.8 pM–4.7 nM	2.2 pM [7.33* pM]	NR	[117]

[a)]NR stands for "not reported"; Values indicated with an asterisk have been calculated from the LOQ or LOD and standard deviation values reported using Equation (1) and (2).

$$\mathrm{LOQ} = \frac{10\sigma}{S} \tag{2}$$

where σ is the standard deviation and S is the sensitivity of the sensor close to zero concentration in Equation (1) and (2).[49]

High-sensitivity nanosensors utilize unique properties of nanotechnology to push the limits of detection of biomarkers below previously achievable concentrations. These high-sensitivity diagnostics can enable earlier detection of diseases to improve patient outcomes. The high surface area to volume ratio allows the detection of biomarkers at extremely limiting amounts such as zepto-(10^{-21}) scales.[43]

6. Diagnostic Modalities and Commercialization in Neurocritical Care

The combination of invasive and noninvasive devices helps clinicians target therapeutic interventions. This section elaborates on the multimodal approach taken, which allows for the effective detection and management of cerebral edema that is specific to the patient pathophysiology.

6.1. Cerebral Tissue Oxygenation

TBI results in a mismatch between the oxygen demand and supply and necessitates continuous real-time monitoring to provide the current state of pathophysiology.[51] Cerebral tissue oxygenation is usually used intraoperatively in intensive care and is coupled with other cerebral invasive and noninvasive monitoring modalities. The jugular venous oxygen concentration ($SjvO_2$) indicates the global cerebral oxygen uptake and is an indicator of the cerebral oxygenation as well as cerebral metabolism.[52] Continuous readings can be obtained via a fibreoptic catheter and the continuous monitoring of $SjvO_2$ is associated with improved patient outcomes and in a normal awake subject is from 55% to 71%.[52]

© 2021 The Authors. Advanced NanoBiomed Research published by Wiley-VCH GmbH

Licox, GMS Integra, allows an invasive measurement of the focal cerebral oxygenation, i.e., brain tissue oxygen tension ($PbtO_2$), in the region of critically perfused brain tissue and is considered superior to $SjvO_2$.[52] $PbtO_2$-based therapy has been associated with 61.2% favorable outcomes, compared to 41.9% using ICP/CPP-based therapy.[53] The system provides clinicians with early warnings of hypoxia, thereby allowing more time to restore oxygen supply. It utilizes a polarographic cell in which oxygen diffuses through the catheter wall into its electrolyte chamber. Oxygen is detected as an electric current when transformed at the electrode. The sampling area is around 14 mm^2.[54] **Figure 3**a gives the cerebral tissue oxygenation as measured by the Licox probe in vivo.

NIRS offers a continuous, noninvasive optical monitoring of brain tissue oxygenation. It is based on the transmission, absorption, and scattering of near-infrared (NIR) light (700–950 nm) in biological tissue.[51] Figure 3b shows the schematic representation of the emission and detection of NIR light. Spatially resolved spectroscopy (SRS) forms the basis of the commercially available cerebral oximeters. The tissue oxygen saturation (TOS) is related to the oxyhemoglobin concentration (O_2Hb) and deoxyhemoglobin concentration (HHb) using Equation (3).[51] SRS forms an array of closely spaced detectors which measure light attenuation as a function of source–detector separation. It implements open and proprietary algorithms to obtain hemoglobin concentration. Examples of commercially available SRS spectrometers include CerOx, Equanox, FORESIGHT, INVOS series, NIRO series and Oxymon Ghosh, Elwell, and Smith.[51] However, NIRS is less accurate when compared to $SjvO_2$.[55] Details of other forms of NIRS are reported by Ghosh et al.[51]

The equation for determination of tissue oxygen saturation (TOS) in spatially resolved spectroscopy is given as follows

$$\mathrm{TOS} = \frac{[O_2Hb]}{[O_2Hb] + [HHb]} \tag{3}$$

Figure 3c shows the decline in the oxygen concentration ($PbtO_2$) with time, which is caused by an increase in the volume of the injury, which serves to occlude the flow of oxygenated blood, as shown by Figure 3d.[56] External remediation strategies are necessary and are duly implemented.

6.2. Cerebral Metabolism

Cerebral microdialysis (CMD) allows bedside invasive and semi-continuous (hourly) monitoring of brain energy supply and analysis of brain tissue biochemistry in the regions that are most susceptible to secondary injury.[52] It allows detection of energetic function through biomarker concentration parameters such as glucose and pyruvate concentration and lactate/pyruvate ratio (LPR); an LRP > 20–25 is associated with poor outcome in TBI.[36,52] In this method, a perfusate solution, typically a normal saline or Ringer's solution, is passed along a semipermeable membrane at the rate of 0.1–2 mL min^{-1} using a pump.[57] The biomarkers present in extracellular fluid (ECF) cross the semipermeable membrane by passive diffusion and enter the perfusate, which can be sampled hourly. This mechanism can be

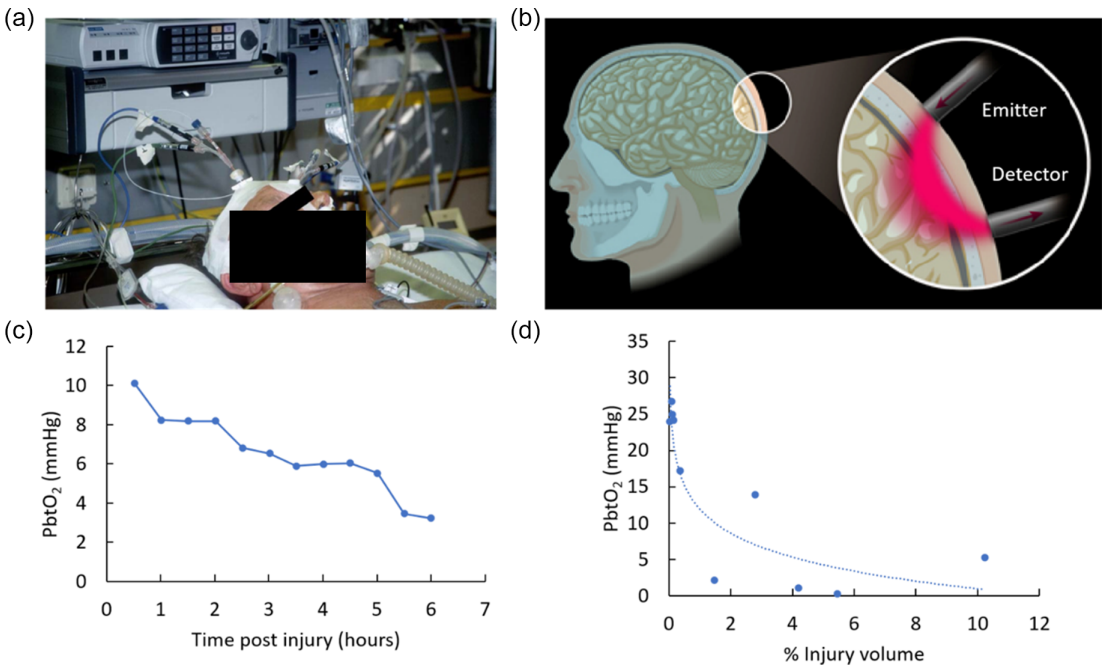


Figure 3. Setup and data for cerebral tissue oxygenation monitoring. a) Application of cerebral tissue oxygenation in a clinical setting. Reproduced with permission.[95] Copyright 2003, mediaTUM. b) The principle of operation of NIRS device where the oxygen concentration in the blood is determined based on the transmission, absorption, and scattering of NIR light. Reproduced under the terms and conditions of the Creative Commons Attribution license 4.0.[96] Copyright 2011, University of Toronto. c) Decline in $PbtO_2$ with increasing time and d) percentage injury volume following TBI. Reproduced with permission.[56] Copyright 2011, the Congress of Neurological Surgeons.

© 2021 The Authors. Advanced NanoBiomed Research published by Wiley-VCH GmbH

26999307, 2021, 11, Downloaded from https://advanced.onlinelibrary.wiley.com/doi/10.1002/anbr.202100001 by Koc University, Wiley Online Library on [05/09/2026]. See the Terms and Conditions (https://onlinelibrary.wiley.com/terms-and-conditions) on Wiley Online Library for rules of use; OA articles are governed by the applicable Creative Commons License

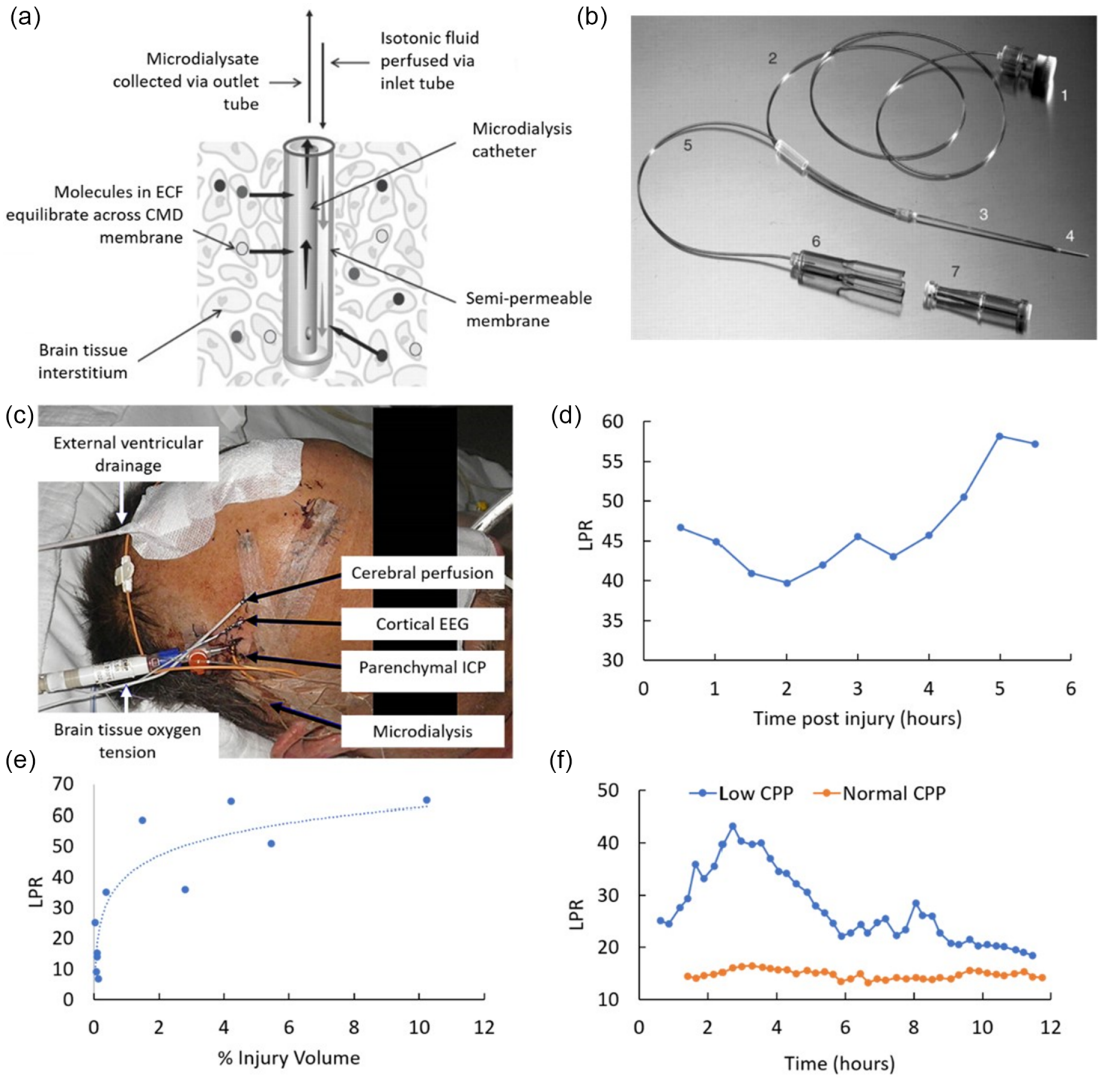


Figure 4. Cerebral metabolism data acquired using microdialysis. a) Schematic representation of the CMD probe. b) CMD probe used in a clinical setting. c) Implementation of the CMD probe in clinical settings. Reproduced under the terms and conditions of the Creative Commons Attribution license 4.0.[97] Copyright 2017, The Authors. d) Increase in LPR with time can be observed following TBI. CMD has not been implemented. e) Increase in LPR with injury volume fraction, which can be seen to level off with time. d), e) are reproduced with permission.[56] Copyright 2011, The Congress of Neurological Surgeons. f) Extensive evolution of LPR with time; the LPR decreases after 3 h once CMD has been implemented. The LPR of the normal case remains stable throughout. a), b), f) are reproduced with permission.[22] Copyright 2006, the Board of Management and Trustees of the British Journal of Anaesthesia.

seen in **Figure 4**a. This fluid is analyzed by either enzyme spectrophotometry or high-performance liquid chromatography.[57] CMD requires the insertion of a specialized catheter (0.62 mm) tipped with a semipermeable dialysis membrane, as shown in Figure 4b,c, into the subcortical white matter. It has a cutoff of 20 kDa.[36]

Alternatively, CMD catheters can be inserted with ICP and $PtbO_2$ probes using a triple lumen bolt, which reduces the risk of catheter displacement. The concentration recorded may be lower than the actual concentration of the ECF, unless a total equilibrium is achieved, which takes prolonged periods.[22,58] Even though CMD is a well-established tool which allows effective management of severe TBI, its use is very limited owing to the cost of implementation.[36,52] Figure 4d shows the elevation in LPR following TBI when no external intervention is implemented. Figure 4e shows the increase and subsequent leveling off of the LPR value following TBI when plotted against the percentage injury volume, which causes hypoperfusion in the brain.[56] Figure 4f shows the temporal evolution of the LPR when CMD is implemented at 3 h and is compared against the baseline case of normal LPR level with no TBI.

6.3. Imaging Techniques

Magnetic resonance imaging (MRI) and computed tomography (CT) are powerful imaging tools in radiology and biomedical

© 2021 The Authors. Advanced NanoBiomed Research published by Wiley-VCH GmbH

26999307, 2021, 11, Downloaded from https://advanced.onlinelibrary.wiley.com/doi/10.1002/anbr.202100001 by Koc University, Wiley Online Library on [05/09/2026]. See the Terms and Conditions (https://onlinelibrary.wiley.com/terms-and-conditions) on Wiley Online Library for rules of use; OA articles are governed by the applicable Creative Commons License

sciences and are used to obtain a snapshot of metabolic changes in the living tissue.[43,59] They allow noninvasive measurements of brain metabolites, especially the biomarkers of injuries. The major advantages of MRI include noninvasive imaging, deep tissue penetration, and superior spatial resolution.[43] However, it suffers from low sensitivity at the cellular and molecular level and hence requires contrast agents for the detection of specific agents; the postprocessing of results obtained is time-consuming.[43] CT is more commonly available due to its speed and relatively low cost and as it can be acutely used. In contrast, MRI is used after the initial injury because of its sensitivity to blood products. MRI works by taking slices of the brain.[60] MRI is also able to distinguish between the different types of edemas. Despite the improvement in the resolution of CT scans, the diagnoses are often nonspecific.[61] CT is unable to detect risk factors for the development of chronic hypoperfusion, which is a cause of edema, and might give false-negative results. As a consequence, CT is not used in the immediate preoperative and postoperative period.[62] Despite the ubiquity of CT scans, they are characterized by poor sensitivity compared to conventional MRI and newer MRI techniques such as proton MR spectroscopy and diffusion tensor imaging are used to detect mild to moderate cases of cerebral edema.[63] Chronic brain atrophy can mask the increased ICP and MRI scanning may be an appropriate tool to alleviate this.[63]

Fluid-attenuated inversion recovery (FLAIR) and diffusion-weighted imaging (DWI) can distinguish between cytotoxic and vasogenic edemas. In FLAIR, an inversion pulse is applied to suppress the high signal emanating from normal fluid-filled spaces such as ventricles and sulci. Although FLAIR is unable to distinguish between cytotoxic and vasogenic edemas following a cerebral insult, it can enhance the visualization of lesions. Additionally, any noticeable changes can only be detected after the first few hours following a neurological insult.[30]

DWI enables the early measurement of changes in the cellular functions in the central nervous system.[64] In DWI, the diffusion of water in the brain tissues is measured, which is detected as apparent diffusion coefficient (ADC) values. Low diffusion corresponds to hypointensities, whereas high diffusion is detected as hyperintensities on the ADC maps. Qualitatively, cytotoxic edemas appear as bright lesions in DWI, whereas vasogenic edemas appear as dark regions on DWI.[30] This can be visualized using **Figure 5**a,b, respectively. Quantitatively, the ratio of FLAIR to DWI < 2 represents cytotoxic edema, but >2 represents vasogenic edema. Proton MR spectroscopy can distinguish between a neoplastic and nonneoplastic brain mass. Further research in the field of molecular imaging will push the boundaries of this field. **Table 6** provides an extensive comparative summary of the latest CT and MRI neuroimaging technologies.

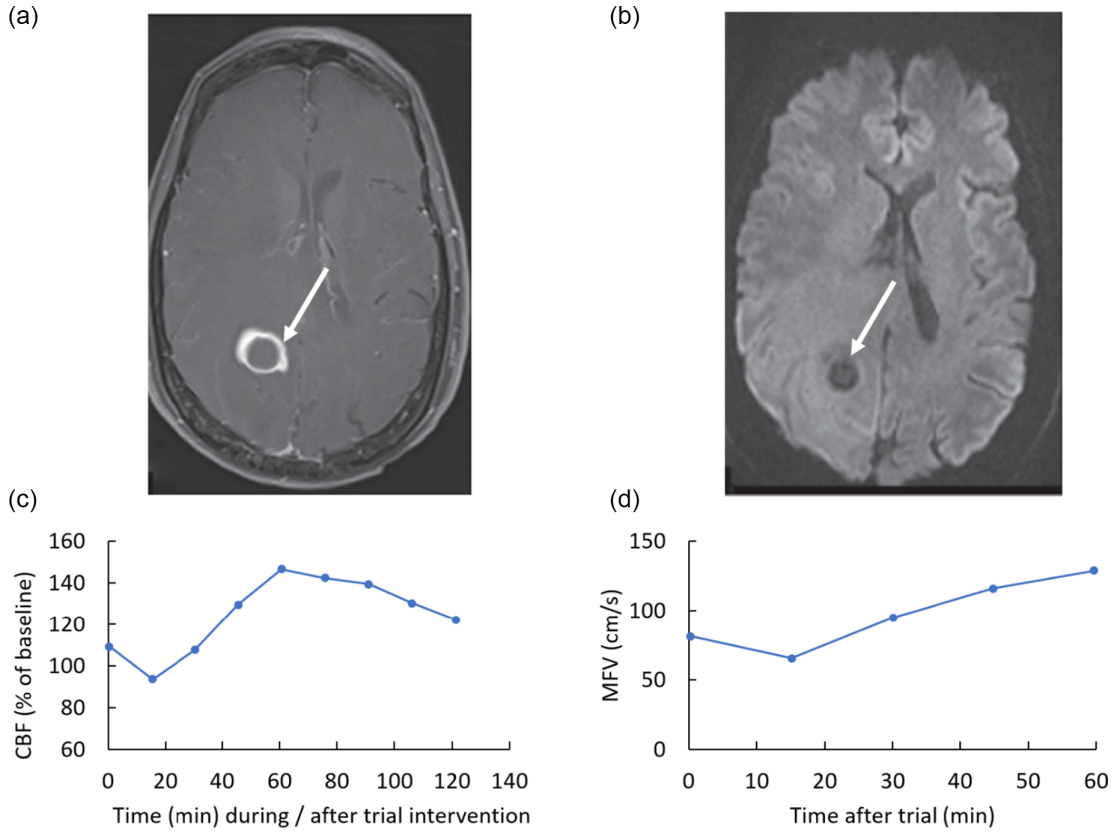


Figure 5. Advanced MRI neuroimaging and CBF data evaluation. a) The arrow shows the region of cytotoxic edema, which appears as a bright spot. b) The arrow shows the location of vasogenic edema, which appears as a dark spot. Adapted with permission.[60] Copyright 2013, Fink KR. c) Variation in CBF and d) MFV with time as measured by TCD. Adapted with permission.[68] Copyright 2016, Springer Nature.

© 2021 The Authors. Advanced NanoBiomed Research published by Wiley-VCH GmbH

26999307, 2021, 11, Downloaded from https://advanced.onlinelibrary.wiley.com/doi/10.1002/anbr.202100001 by Koc University, Wiley Online Library on [05/09/2026]. See the Terms and Conditions (https://onlinelibrary.wiley.com/terms-and-conditions) on Wiley Online Library for rules of use; OA articles are governed by the applicable Creative Commons License

26999307, 2021, 11, Downloaded from https://advanced.onlinelibrary.wiley.com/doi/10.1002/anbr.202100001 by Koc University, Wiley Online Library on [05/09/2026]. See the Terms and Conditions (https://onlinelibrary.wiley.com/terms-and-conditions) on Wiley Online Library for rules of use; OA articles are governed by the applicable Creative Commons License

Table 6. Advantages and disadvantages of conventional and advanced CT and MRI imaging techniques[a)]

	Advantages	Disadvantages
Nonenhanced computed tomography (NECT)	First-line imaging modality Easy to obtain and well tolerated Excludes life-threatening emergencies	Insensitive; necessitates further imaging
Contrast-enhanced computed tomography (CECT)	Enhances results from NECT More sensitive to noncontrast MRI Alternative to conventional MRI Used for contradictory MRI	Less sensitive than contrast-enhanced MRI
Proton magnetic resonance spectroscopy (MRS)	Allows spectroscopic differentiation of several biomarkers Allows distinguishing edema and neoplasms	Variable biomarker concentration ratios: thresholds are advisory
Contrast-enhanced magnetic resonance perfusion (MRP)	Visualizes elevated blood flow levels Differentiates between metastases and cerebral abscess	Gadolinium-based substances allow contrast imaging
Diffusion-weighted imaging (DWI)	Depicts facilitated diffusion as bright spots Can distinguish between hypoxic–ischemic injury and focal infarction Used as a tool for assessing the efficacy of neuroprotective agents	Imaging restricted to three directions only
Diffusion tensor imaging (DTI)	Allows detailed imaging in six directions Early detection of brain edema during hypoxic–ischemic reperfusion More sensitive than conventional MRI	ADC value varies and decreases with age
Fluorodeoxyglucose positron emission tomography (FDG PET)	The cerebral cortex is sensitive to FDG PET	Not as sensitive as MRI scans Only 27% sensitive compared to CEMRI

[a)]Data obtained from ref. [10] and ref. [60].

6.4. Cerebral Blood Flow (CBF)

CBF allows continuous point-of-care monitoring to provide a better understanding of the cerebral perfusion and is seen as the most important biomarker for fuel delivery.[57,65] Transcranial doppler (TCD) is a continuous, noninvasive method to determine cerebral blood flow (CBF) velocity.[52] This technique utilizes the Doppler shift principle to obtain the red blood cell mean flow velocity from pulses of high-frequency ultrasound waves which are aimed at basal cerebral arteries; the reflection causes a change in direction and velocity, which is used to determine the CBF.[65,66] The overall sensitivity of TCD for determining brain death is 75–88% and the overall specificity is reported to be 98%.[52] However, TCD is unable to distinguish between the symptomatic and asymptomatic measurements ranging at velocities between 120 and 199 cm s^{-1}.[57]

QFlow 500 Perfusion Probe, Hemedex, permits regional monitoring of the cerebral flow rate by assessing thermal convection due to tissue blood flow. It is fully flexible and biocompatible with a diameter of 1 mm.[67] It has an apparent lower limit of 15 mL/100 g min^{-1} and recordings below this limit are less reliable. This device is not MRI-compatible and it is radiologically opaque.[57,67] The probe is fixed in place using a skull bolt to avoid catheter dislodgement. The probe is inserted 1–1.5 cm anteriorly into the white matter and generally next to ICP/$PbtO_2$ probes.[36,57]

Figure 5c,d shows the results obtained using TCD in CBF monitoring using data obtained from Westermaier et al.[68] The results show global CBF recovery after a period of hypoventilation caused by hypercapnic intervention and the reinstatement of the basal oxygen level as measured by TCD. The MFV shows an increase, while the CBF% is seen to recover to basal levels.

6.5. Brain Electrical Activity

The electrical activity of the cerebral cortex can be studied to uncover the underlying pathophysiology. Electroencephalography (EEG) mainly results from the summation of postsynaptic currents of pyramidal cells in the cortical brain layers.[69] The lower limit to the spatial resolution of scalp EEG is determined by the 40 mm^2 of the active cortex and is of the order of 10 nA, which is essentially the summation of the current generated by around a million pyramidal cells, with each generating 20 fA current.[70] The electrical activity is detected using electrodes that are attached to the scalp and it is a safe and noninvasive technique. Although EEG is classically used to indicate seizures caused by epilepsy, nonconvulsive seizures may be associated with secondary cerebral damage and tissue loss such as elevated ICP, cerebral ischemia, and edema.[71] Cerebral edema is a complication that can be detected during intracranial EEG monitoring using continuous EEG (cEEG).[26,71] Any irregularities in ICP can be detected by cEEG prior to other clinical findings (even before the emergence of symptoms), which enables early interventions. A minimum of 2 days of cEEG is required to detect nonconvulsive seizures with more than 90% sensitivity.[57]

Figure 6 shows the electrode-based EEG systems in clinical settings (a), 128 electrode system by Compumedics Neuroscan (b).[72]

 © 2021 The Authors. Advanced NanoBiomed Research published by Wiley-VCH GmbH

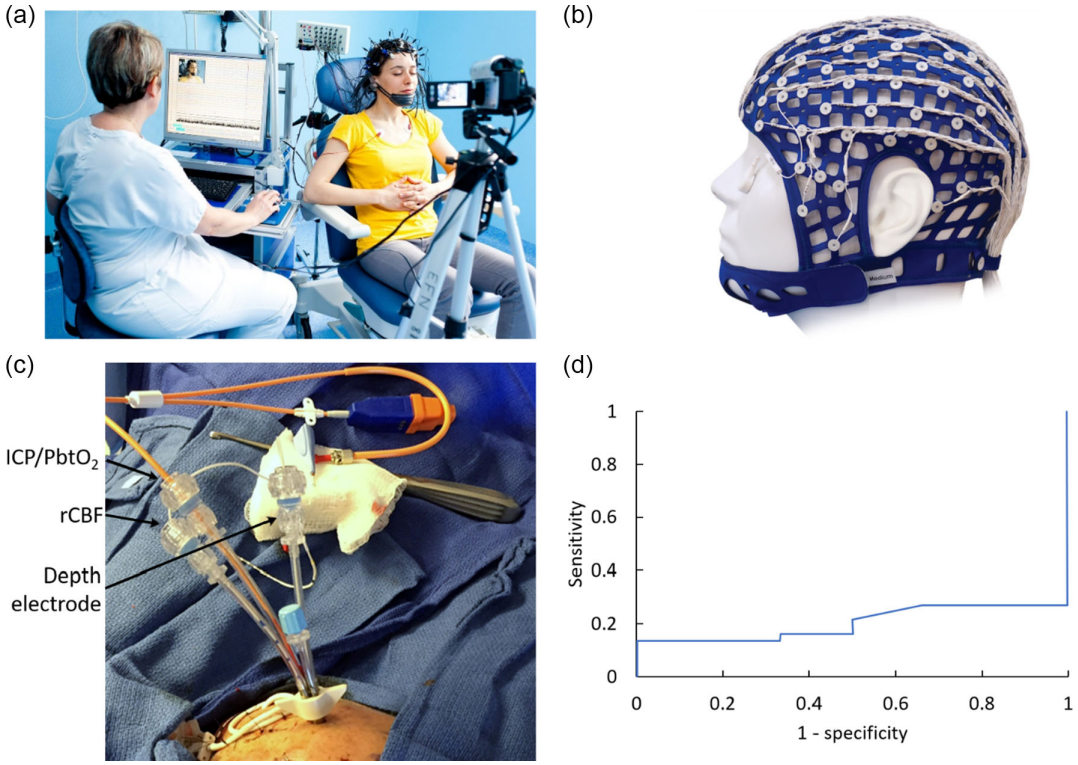


Figure 6. The scale of implementation of the electroencephalography (EEG) and ICP monitoring systems. a) EEG systems implemented at point of care. Reproduced with permission.[98] Copyright 2018, Crown. b) Compumedics Neuroscan 128 electrode EEG system (Compumedics Neuroscan, no date). Reproduced with permission. Copyright 2021, Compumedics Neuroscan. c) In vivo implementation of the ICP catheter. Reproduced with permission.[99] Copyright 2019, MyJoVE Corporation. d) Plot of sensitivity against 1-specificity for an ICP catheter. Reproduced with permission.[100] Copyright 2013, Informa UK Limited.

6.6. Intracranial Pressure Monitoring

The Monro–Kellie hypothesis dictates that the human skull is inelastic and has a finite volume of 1700 mL. Its three constituents are the brain matter (1400 mL), CSF (150 mL), and blood (150 mL). An increase in either of these components due to primary and secondary injuries induced by TBI causes compressive stress on the surrounding components and elevates the ICP.[73,74] Cerebral edema manifests itself as an increase in the ICP due to fluid retention in the brain tissue.[57,75] This fluid build-up causes an inflammatory reaction in the surrounding tissue in the form of swelling due to the body's natural response to an injury. Although the source of the fluid has been debated, CSF has now been identified as the primary source of edema fluid by Mestre et al.[75] Elevated ICP can restrict the flow of oxygenated blood to the brain, and the lack thereof causes hypoxia. This damages the brain cells and renders them irreparable; fatality is possible in some cases. ICP can have a regional or global impact depending on the underlying cause, but clinical experiences inform that a global increase in ICP begins as regional edema.[57]

Cerebral perfusion pressure (CPP) drives the blood through the blood capillaries, which is a clinically available measure in TBI and is the difference between the mean arterial blood pressure (MAP) and ICP. This is represented mathematically by Equation (4).[76]

The relationship between CPP, MAP, and ICP to explain edema development is shown as follows

$$\mathrm{CPP} = \mathrm{MAP} - \mathrm{ICP} \tag{4}$$

Although the MAP remains relatively constant, an elevated ICP may decrease the CPP and restrict blood flow. This deprives the brain of oxygen and causes the brain to respire anaerobically by exhausting the glucose supply. This also releases stress biomarkers.[76] To treat the secondary injury, the CPP can be increased to restore CBF and thereby increase oxygenation to the target tissue. However, loss of autoregulation may cause the intracranial pressure to increase, causing herniation.[6] Alternatively, neuroprotectants such as beta-adrenergic blockers, alpha one agonists, barbiturates, and sedatives are used to selectively target the reduction in ICP instead of elevating the CPP.[6] The CSF can be drained counter edema formation and may be coupled with osmotic diuretics to drain the excess water. Additionally, CPP can also be increased by increasing MAP using vasopressors.[6]

Raised ICP can be attributed to a 3.5–6.9 fold increase of death compared to normal ICP levels.[36] The external ventricular drains are deemed "gold standard" and allow the simultaneous measurement and drainage of CSF, whereas subarachnoid and epidural ICP monitors have limited accuracy.[76] Despite their accuracy, invasive ICP monitoring is prone to bleeding, infections, and CSF leakage.[1,38,77] Several ICP probes have been

© 2021 The Authors. Advanced NanoBiomed Research published by Wiley-VCH GmbH

26999307, 2021, 11, Downloaded from https://advanced.onlinelibrary.wiley.com/doi/10.1002/anbr.202100001 by Koc University, Wiley Online Library on [05/09/2026]. See the Terms and Conditions (https://onlinelibrary.wiley.com/terms-and-conditions) on Wiley Online Library for rules of use; OA articles are governed by the applicable Creative Commons License

commercialized, including Codman MicroSensor, Raumedic, Neurovent, and Camino Integra, which are all invasive in nature. Transcranial doppler (TCD) provides a noninvasive evaluation of elevated ICP, but not monitoring capabilities.[36] Flow velocities in the middle cerebral artery are used to detect a drop in TCD-derived flow velocity, which is indicative of elevated ICP.[78] Figure 6c shows the implementation of ICP measurement in vivo. Figure 6d shows the graph of sensitivity against 1-specificity for the ICP probe.

6.7. Comparison of Diagnostic Modalities in Neurocritical Care

Table 7 provides a succinct summary of several techniques used in the diagnosis and treatment of cerebral edema and lists their advantages and disadvantages.

7. Promising Technologies for Managing Cerebral Edema

Vital information on the compositional dynamics of biological tissues and underlying pathophysiology can be obtained by assessing several modalities, which is exploited by means of advanced devices.

Developed over half a century ago, bioelectrical impedance measurements are used to detect water content and edema. Electrical impedance tomography (EIT) uses contact electrode measurements to image to produce a map of the electric impedance of tissue for use in various medical imaging applications, such as for the detection of edema. Alternatively, noncontact electrical coils can be used to accomplish the same thing using volumetric electromagnetic phase shift spectroscopy (VEPS).

7.1. Volumetric Electromagnetic Phase Shift Spectroscopy (VEPS)

The VEPS technology provides an inexpensive diagnostic tool for medical imaging as VEPS can noninvasively detect changes in tissue properties without any contact using multifrequency electromagnetic measurements that originate externally. The skull is transparent to the magnetic field, which enables the probing of the underlying brain tissue. VEPS can distinguish between healthy individuals and those with a brain condition using low-frequency electromagnetic (EM) waves ranging from 26 to 39 MHz, and between brain edema and hematoma using high-frequency EM waves ranging from 153 and 166 MHz, with a statistical significance of $p < 0.05$ in both cases. The ability to distinguish edema from hematoma is important and occurs owing to the sensitivity of VEPS.[79]

The theoretical study using a pig brain in vitro was confirmed to prove the effectiveness of VEPS in detecting edema. A

Table 7. Summary of diagnostic modalities in neurocritical care.

Technique[a)]	Modality	Unit	Resolution	Advantages	Disadvantages
$PbtO_2$	Cerebral tissue oxygenation	Torr	Low spatial, high temporal resolution	Local presence of oxygen Direct measurement of brain tissue content	Invasive technique Regional as opposed to global changes
$SjvO_2$	Cerebral tissue oxygenation	Torr	NR	Global oxygen presence Continuous and real-time measurements Low cost	Invasive technique Limited use of time Incorrect reading due to tip movement
NIRS	Cerebral tissue oxygenation	%	Low spatial, high temporal resolution	Noninvasive Continuous, real-time bedside monitoring Indicates local perfusion	Difficult to interpret in edema Sometimes unclear extracranial contribution
CMD	Cerebral metabolism	mmol L^{-1}	Low spatial, moderate temporal	Local cerebral metabolism Identification of key biomarkers	Value dependent on proximity to lesions Invasive Requires hourly assessment
TCD	Cerebral blood flow	cm s^{-1}	Low–moderate spatial, moderate–high temporal	Noninvasive Global perfusion Point-of-care assessment	Absence of vessel diameter information, so cannot assess absolute flow
cEEG	Brain electrical activity	NR	Low–moderate spatial, high temporal	Diagnosis of seizures Sensitive to encephalopathy and ischemia monitoring	Lack of neuroanatomical visualization Requires training for the interpretation
External ventricular drain	ICP	mmHg	Low–moderate spatial, high temporal	Global ICP measurements Continuous monitoring capabilities	Increased infection risk Difficult placement in effaced ventricles Needs clamping to measure ICP
Intraparenchymal ICP monitor	ICP	mmHg	Low spatial, high temporal	Continuous measurements Indication edema evolution Easy placement Low infection risk	ICP gradient complicates interpretation Drift in units over time No therapeutic benefit Cannot be recalibrated in vivo

[a)]Adapted from ref. [42], ref. [118], and ref. [66]; NR = not reported. Please refer to Table 6 for an extensive comparison of the various imaging techniques.

© 2021 The Authors. Advanced NanoBiomed Research published by Wiley-VCH GmbH

26999307, 2021, 11, Downloaded from https://advanced.onlinelibrary.wiley.com/doi/10.1002/anbr.202100001 by Koc University, Wiley Online Library on [05/09/2026]. See the Terms and Conditions (https://onlinelibrary.wiley.com/terms-and-conditions) on Wiley Online Library for rules of use; OA articles are governed by the applicable Creative Commons License

numerical study involving a circular and magnetron sensor coils has shown the capability of detection of brain hematomas using VEPS. A simulation study confirmed the differentiating ability of VEPS between hypoperfusion and bleeding. The experimental design of the VEPS suitable for humans was tested on a spherical head simulation model.[79]

The VEPS device shown using **Figure 7**a,b,d shows its implementation in a clinical setting. The device consists of an inducting coil and a sensory coil. These coils are coaxial, and the head is placed between these two coils. An alternating current in the inductor coil generates a primary magnetic field that interacts with the enclosed brain tissue volume, which in turn produces a perturbation of the primary magnetic field. The change in the magnetic field represents volumetric changes in the brain composition complex impedance. These can be easily detected using a phase shift between the inductor and sensory coil. The phase difference is used to estimate the VEPS.[79] The author stresses the importance of the development of a VEPS database to enable seamless classification of diagnostic capabilities; however, it is acknowledged that this is a laborious but essential next step to unlock future modalities.[79] Figure 7c shows the plot of electrical conductivity against the variation in frequency.

7.2. Osmotic Transport Device (OTD)

An OTD is used to reduce cerebral edema following TBI by allowing direct extraction of water from the edematous tissue using direct osmotherapy using a hydratable material for water extraction by osmotically driven flux.[80] Their study includes a schematic for the placement of the device in vivo. This study was performed on mice models, where TBI was induced using controlled cortical impact (CCI) and edema could form for 3 h and the subsequent treatment followed for 2 h. When treated, the brain water content was not significantly higher than that of the control group.

This is a very invasive process and requires a craniectomy or burr hole to access the contusion. A lumen solution flows through the hollow fibers at a flow rate such that the Reynolds number is between 50 and 100. Bovine serum albumin was used as the osmotic agent because its concentration-dependent osmotic pressure range is well known, and its concentration-dependent viscosity is manageable.[80] Their results show the variation in the brain water content in the left and right cerebrum and the cerebellum after a variety of approaches were taken. The hollow fibers allow the movement of water and ions from the brain but restrict the motion of the osmotic agent. The highly permeable hydrogel helps to maintain good contact. The advantage of this method is that it does not dehydrate the surrounding tissue as equilibrium is established. While this allows for a reduction in the brain water content, it is unknown whether this leads to an improvement in neurological outcome. So, larger animal models are needed for this purpose. As mice brains are 3000 times smaller than a human brain, massive scale-up efforts will be needed for the utilization of this technique for humans.[80]

7.3. Coaxial Probe (CoaxP)

Inspired by the need to quantify edema for autopsies after a person's death, the coaxial probe provides effective diagnostic capabilities. This method allows rapid and cheap measuring

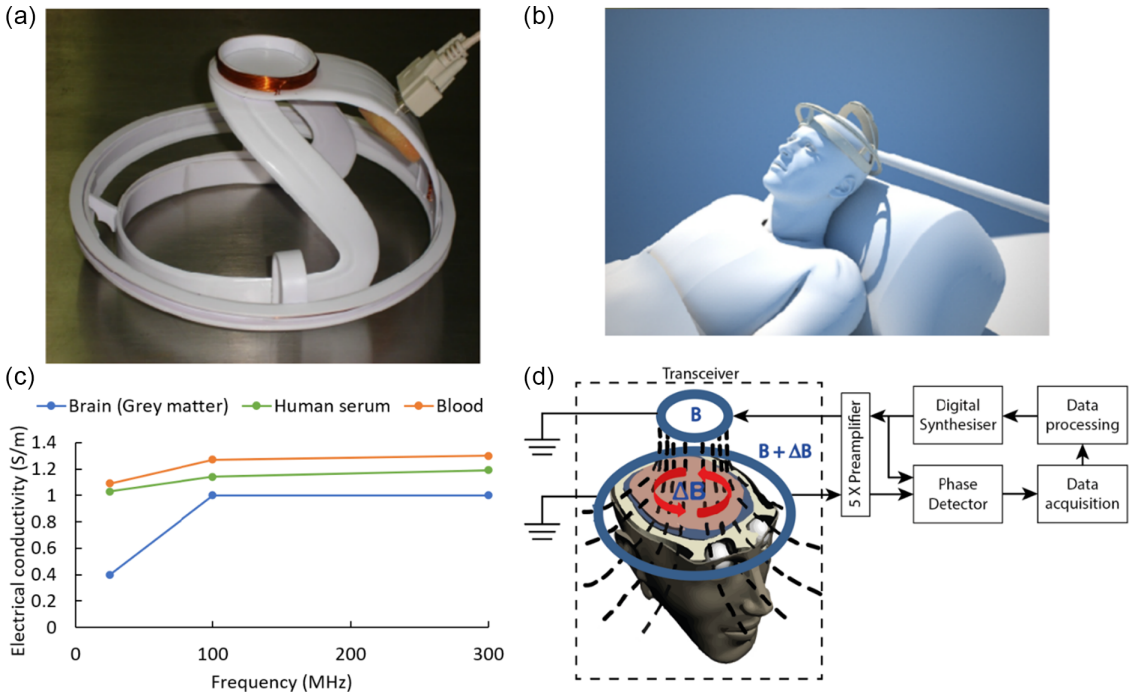


Figure 7. VEPS scan set up to measure the phase shift. a) The VEPS headset designed by Gonzalez et al.[79] Reproduced under the terms and conditions of the Creative Commons Attribution license.[79] Copyright 2013, The Authors, published by PLOS. b) Application of VEPS in vivo. c) Plot of electrical conductivity against frequency.[79] Reproduced under the terms and conditions of the Creative Commons Attribution license.[79] Copyright 2013, The Authors, published by PLOS. d) Block diagram depicting the application of the VEPS technology in humans.

© 2021 The Authors. Advanced NanoBiomed Research published by Wiley-VCH GmbH

26999307, 2021, 11, Downloaded from https://advanced.onlinelibrary.wiley.com/doi/10.1002/anbr.202100001 by Koc University, Wiley Online Library on [05/09/2026]. See the Terms and Conditions (https://onlinelibrary.wiley.com/terms-and-conditions) on Wiley Online Library for rules of use; OA articles are governed by the applicable Creative Commons License

capabilities for autopsy, which could be used for in vivo diagnostics.[81] Two methods were tested, including transmission ($R = 0.97$) and reflection ($R = 0.98$); however, for in vivo monitoring, the transmission method is unsuitable. Although humidity is deemed as an effective tool to contrast between different causes of death, there is no current consensus on an effective technique to determine the moisture content.[81] The reflection method is of interest as it implements an open-ended coaxial probe for the nondestructive determination of permeability. This is shown by **Figure 8**a–c. The probe measures the permittivity of the brain sample from reflection when pressed against the brain, and the results are calibrated using the moisture analyzer.[81] The results of the permittivity as a function of the brain water percentage is shown by Figure 8d. This avoids the need to take out a sample and offers a promising solution for its applications in patients. The humidity content in the brain was shown to vary from 65% to 90%; however, this was for a cadaver. The measuring time is about 20 s, which is very quick and uses electromagnetic radiation with an electric field of frequency 500 MHz. There is a good agreement with the theoretical values and the measured permittivity hence highlights the probe's accuracy. The major drawback of the reflection method is that the specimen must always remain in good contact with the probe. Else, air bubbles form, which reduce the surface of contact and produce an underestimate for the permittivity. The high contact pressure can induce stress on the underlying tissue and force water to leak, causing a lower permittivity—that for water.[81] However, this is limited to the anatomy of the deceased brain and may not be reflected in the surviving brain. The maximum error in the measurement is 3% for the maximum theoretical humidity of 99.1%. However, the humidity data are variable between any two points, so the data validation is only transiently accurate and at the stated location.

7.4. Coplanar Probe (CopP)

This method is an improvement on the previous method and functions along the same principles which are prone to an error in measurements due to a variation in contact pressure, which has an impact on the permittivity of the brain tissue. The device was calibrated against commercial food grade moisture analyzers, which are characterized by high accuracy (standard deviation of 0.5 wt%) and takes ≈10 min, which is deemed time-consuming in a routine autopsy. Consequently, a nondestructive method relying on measuring the permittivity of brain tissue was developed, which provides quicker results. The permittivity of the tissue is determined by pressing the sample onto the brain tissue and the transmission of an electromagnetic wave is measured. **Figure 9**a–c shows the coplanar device used for brain tissue, the basic schematic of the device, and the base of the actual probe, respectively.[82]

The effective permittivity is determined by measuring the phase shift of the transmitted electromagnetic wave, which then enables the determination of the water content and thus the extent of edema. Figure 9d shows the plot of permittivity against brain water content. However, the author acknowledges that the sensor could be implemented in vivo upon sterilization.[82]

7.5. Portable Microwave-Based Systems (PMBSs)

Microwave radiation is nonionizing radiation and has attracted the attention of researchers as a low-cost and low-power

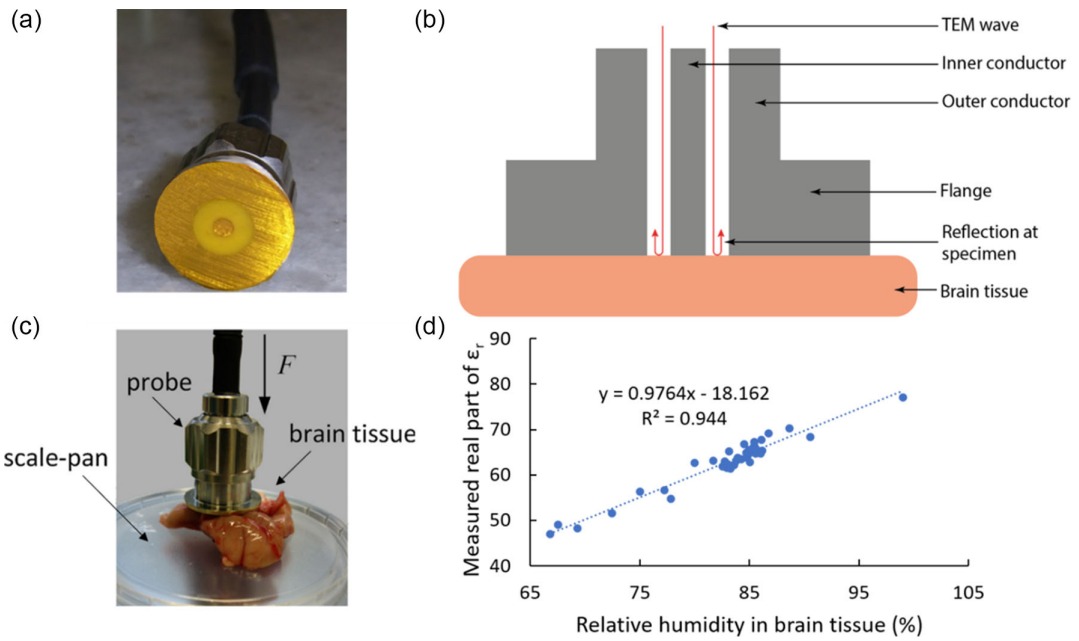


Figure 8. Coaxial probe for the measurement of brain permittivity to determine the extent of edema. a) Image of the base of the coaxial probe that meets the brain tissue. b) Schematic of the coaxial probe for the measurement of brain permittivity. Adapted with permission.[81] Copyright 2014, Elsevier B.V. c) Coaxial probe used to measure permittivity with $0.2 < F < 1$ N. d) Plot of relative permittivity against relative humidity in the brain tissue in percentage. Adapted with permission.[81] Copyright 2014, Elsevier B.V.

© 2021 The Authors. Advanced NanoBiomed Research published by Wiley-VCH GmbH

26999307, 2021, 11, Downloaded from https://advanced.onlinelibrary.wiley.com/doi/10.1002/anbr.202100001 by Koc University, Wiley Online Library on [05/09/2026]. See the Terms and Conditions (https://onlinelibrary.wiley.com/terms-and-conditions) on Wiley Online Library for rules of use; OA articles are governed by the applicable Creative Commons License

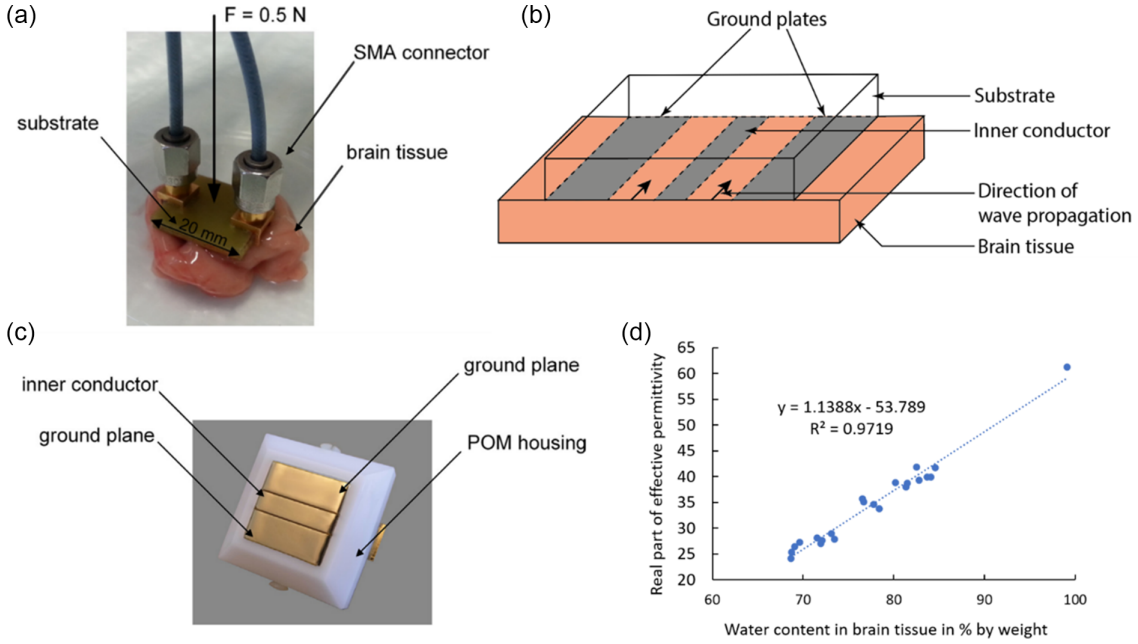


Figure 9. Coplanar probe for the measurement of brain permittivity to determine the extent of edema. a) The use of the coplanar probe for a tissue sample. b) Schematic of the coplanar probe. Adapted with permission.[82] Copyright 2015, Elsevier B.V. c) Bottom surface of the coplanar probe. d) Plot of effectivity permittivity against brain tissue water content used to determine water content in autopsy. Adapted with permission.[82] Copyright 2015, Elsevier B.V.

diagnostic tool for noninvasively detecting cerebral edema. Edema manifests itself as an accumulation of fluid in the brain tissue, which causes a change in the conductivity due to the presence of edema.[83] This property is exploited in the novel microwave-based head detection system that allows the continuous assessment of edema. Its effectiveness was demonstrated using anatomically and dielectrically similar dummy models consisting of regions of skin, cranium, gray matter, white matter, and cerebral edema.[83] **Figure 10**a shows a schematic of the edema detection system. This prototype consisted of a circular waveguide, which acts as the detector, a coaxial cable used to transmit and receive microwave signals, and a vector network analyzer (VNA), which helps to store and process data. The matching medium enables a good electromagnetic coupling between the sensor and the head tissue. Different volumes of cerebral edema were tested ranging from 1 to 20 mL and the experimental frequency range of the wave group ranged from 150 to 450 MHz.

Figure 10b shows the amplitude plotted for different edema volumes, which was used to produce Figure 10c, which shows the amplitude shift plotted against edema volumes obtained for the second significant peak, which shows a good fit between the amplitude shift and edema volume values as judged by the R^2 value of 0.9971. A greater change in the amplitude corresponds to a small yet distinguishable shift in the conductivity of the dummy models, which decreases with increasing volumes of edema. Therefore, the power of the microwave signal decreases due to the conductivity loss; this finding could be exploited for the real-time monitoring capabilities of measuring rate and size of edema expansion in clinical environments.

7.6. EIT

EIT is a noninvasive imaging tool for monitoring the onset of cerebral edema. Cerebral fluids, such as CSF, contain ions that are conductors. Cerebral edema can cause excessive accumulation of these fluids and disrupt their homeostatic concentrations. Therefore, cerebral edema affects the impedance of brain tissue, and thus enables the use of EIT as a potential monitoring tool.[12]

EIT uses an array of 16 contact electrodes to inject harmless currents in the body and measure voltage to produce a map of the electric impedance of tissue for use in various medical applications, as shown by **Figure 11**b. The EIT system can produce alternating current signals from 500 to 1250 μA with a working frequency of 1–190 kHz and a signal-to-noise ratio of >89 dB. The voltage difference can be precisely measured. In this study, a safe alternating current (1 mA–50 kHz) was applied through pairs of electrodes opposite each other, and voltages on other adjacent electrode pairs were measured, as shown in Figure 11d.

EIT has been demonstrated successfully in animal tests, including the detection of intraventricular hemorrhage in neonatal piglets. The noninvasive measurements of cerebral impedance were highly correlated with ICP. Additionally, EIT was combined with ICP sensors to detect induced trauma in intraparenchymal hemorrhage in animal models. In humans, it has been applied in clinical real-time monitoring of lung ventilation and perfusion, although the application in brain perfusion was lacking. To address this, the feasibility of EIT to track the development of cerebral edema was examined in a study by Yang et al.[12] The sample size was 40 and only patients with the cerebral hemorrhage who required ICP monitoring were included in the study.

© 2021 The Authors. Advanced NanoBiomed Research published by Wiley-VCH GmbH

26999307, 2021, 11, Downloaded from https://advanced.onlinelibrary.wiley.com/doi/10.1002/anbr.202100001 by Koc University, Wiley Online Library on [05/09/2026]. See the Terms and Conditions (https://onlinelibrary.wiley.com/terms-and-conditions) on Wiley Online Library for rules of use; OA articles are governed by the applicable Creative Commons License

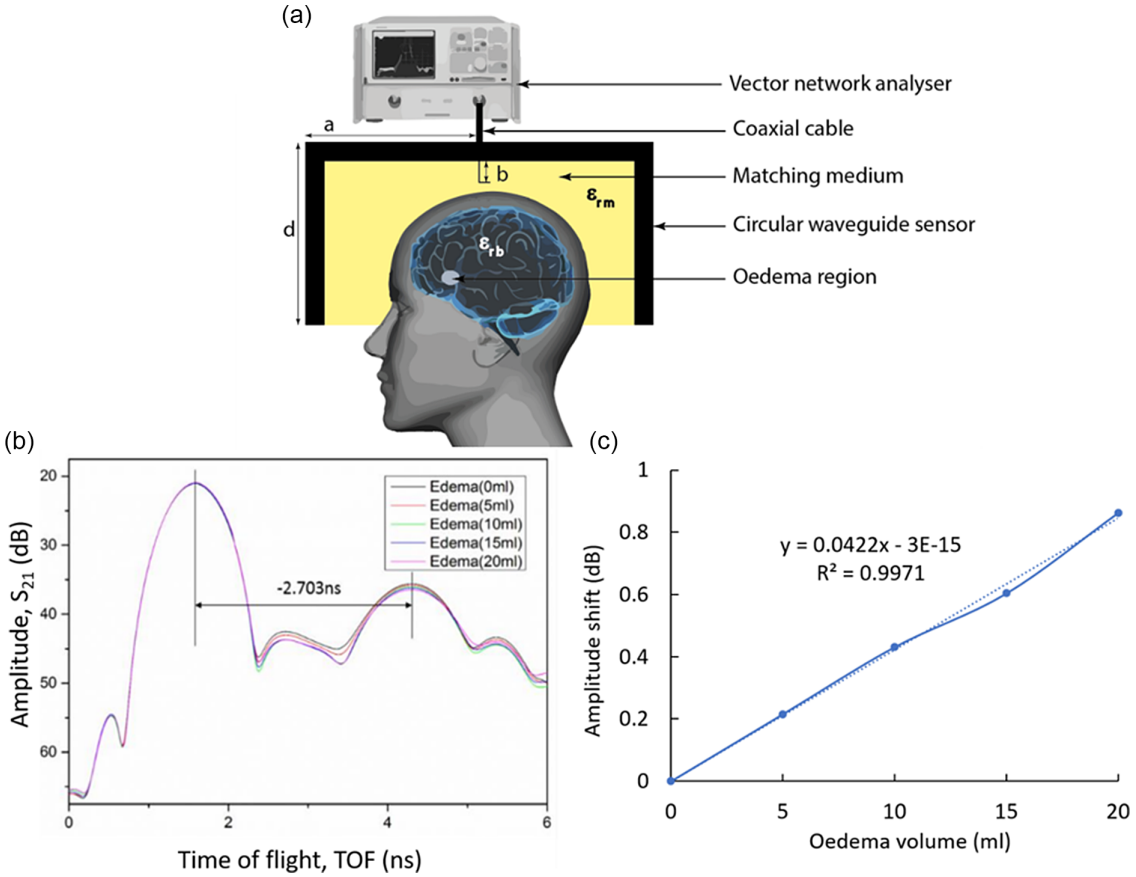


Figure 10. PMBS to detect the presence of cerebral edema. a) Schematic of the PMBS system for the noninvasive detection of cerebral edema. b) The plot of amplitude (in dB) against the time of flight for the different edema volumes. The amplitude is seen to decrease with the increasing edema volumes.[83] c) The plot of amplitude shift (in dB) against edema volume (in mL). The amplitude shift is calculated from the baseline case where the amplitude is obtained for the 0 mL case of edema. Adapted with permission.[83] Reproduced under the terms and conditions of the Creative Commons Attribution license 3.0. Copyright 2018, The Authors, published by IOP Publishing.

The dynamics of the brain dehydration using mannitol was examined. The dehydration of the brain tissue can reduce ICP by establishing an osmotic gradient between the brain tissue and blood. Hence, mannitol treatment was monitored through EIT to explore the feasibility of monitoring cerebral edema. The impedance imaging of the brain with regard to the water content is correlated with the ICP readings. Hyperosmolar therapy with mannitol was shown to decrease the ICP and increase the brain impedance with a highly negative correlation between the ΔICP and average reconstructed impedance value (ΔARV) ($R2 = 0.78 \pm 0.16$, $p < 0.001$), with a similarity of 92.5%. Figure 11a shows the variation in the ICP (left axis) and mean resistivity value (right axis) with time. The mean resistivity value increases when mannitol administration is commenced.

The major drawbacks of this study are that the readings of EIT and ICP are sensitive to the patient movement. The spatial resolution and impedance sensitivity of the EIT system are spatially nonuniform and worsen toward the center of the imaged region. The scalp impedance may have an impact on the EIP measurements during rehydration, which must be taken away from the brain impedance readings. The sensitivity reported was 65% and specificity was 70% for the ICP changes greater than 10 mmHg, which suggested the effectiveness of EIT caused by elevated ICP to a certain degree. This technology has the potential to enable early identification of cerebral edema (**Table 8**).[12]

8. Treatment of Cerebral Edema Using Neuroprotective Agents

Clinicians have previously attempted to treat stroke patients through neuroprotective agents such as oxygen radical scavengers, *N*-methyl-D-aspartate (NMDA) receptor antagonists, and matrix metalloprotease (MMP) inhibitors. However, less than satisfactory results were obtained.[84] This has further necessitated effective neuroprotective therapeutics and some of these have been highlighted subsequently. However, this review does not attempt to exhaustively cover these. The following neuroprotectants have worked in principle to mitigate, or in some cases reverse, the damage caused by TBI or other causes of cerebral edema. Those which are currently in clinical trials have been covered comprehensively here.[85] If therapeutic interventions are applied during the onset of the disease, the predisease cerebral function may be reinstated.[71]

© 2021 The Authors. Advanced NanoBiomed Research published by Wiley-VCH GmbH

26999307, 2021, 11, Downloaded from https://advanced.onlinelibrary.wiley.com/doi/10.1002/anbr.202100001 by Koc University, Wiley Online Library on [05/09/2026]. See the Terms and Conditions (https://onlinelibrary.wiley.com/terms-and-conditions) on Wiley Online Library for rules of use; OA articles are governed by the applicable Creative Commons License

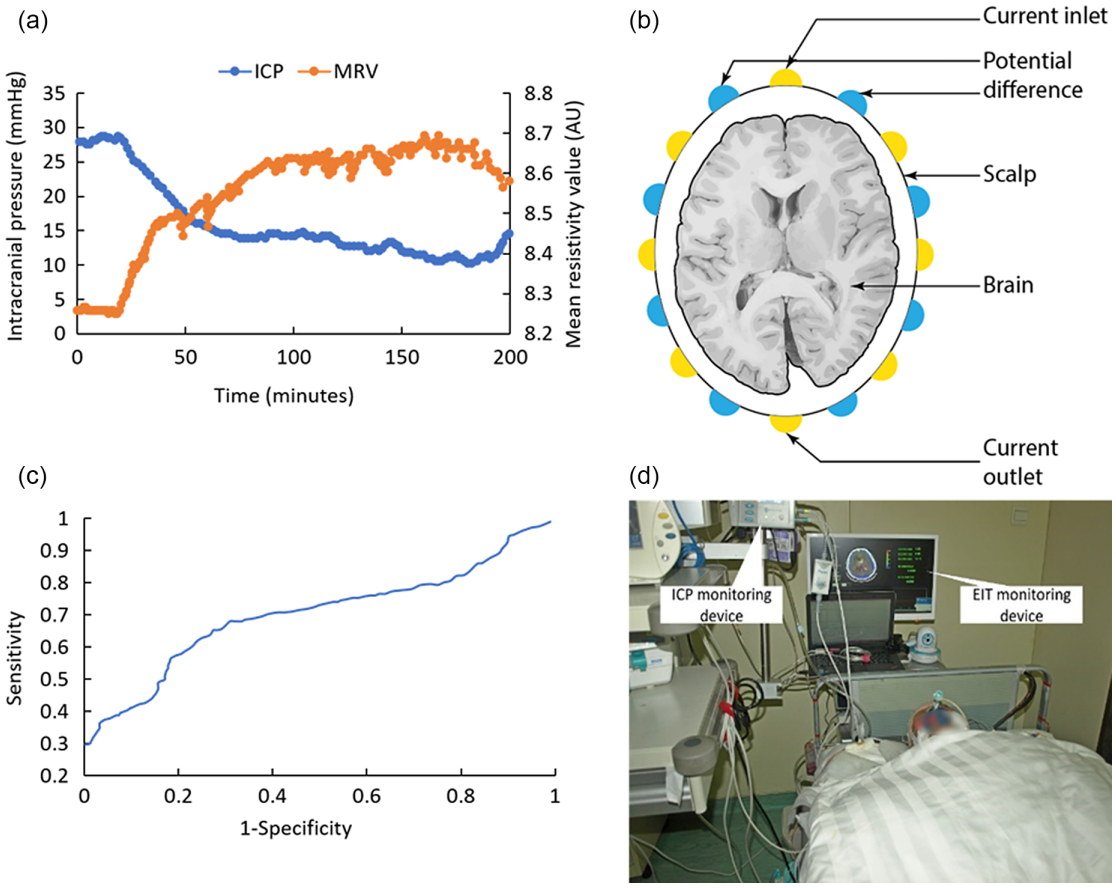


Figure 11. Pertinent figures for the use of EIT to detect cerebral edema. a) Timeline of the experiment after the administration of mannitol. Raw and mean intracranial pressure data (top). Mean of the raw resistivity values (middle). Change of average reconstructed impedance value (ARV) compared to reference data calculated from EIT images (bottom). b) Schematic of the proposed EIT device. c) Plot of sensitivity against 1-specificity for the proposed device. d) Setup on the EIT monitoring device in the clinic. Reproduced with permission.[12] Copyright 2019, The Authors, published by Elsevier Inc., some rights reserved.

8.1. Taurine

Taurine (1-aminoethane sulfonic acid) is an important nonprotein amino acid that exists in neurons in free form and aids in brain growth and development. It aids in neuroprotection and regeneration after injuries in the nervous system as it acts as an osmoregulator, neuromodulator, calcium regulator, and offers neuroprotection against excitotoxic cell death.[16,47] Supplementing recovery of TBI patients has been demonstrated successfully with taurine, particularly in rat models, where it was shown to reduce neurological deficits and lessen brain swelling.[16] Taurine treatment was shown to improve CBF by lowering edema and brain inflammation and had negligible variations from the normal state after 7 days of taurine treatment.

The inflammatory response following TBI involves several steps, including the secretion of cytokines. In another study involving 72 lab rats, taurine was shown to improve neurological function by causing a reduction in cerebral edema.[47] TBI led to an increase in cytokine concentration and water content compared to the shams group.[47] There was a marked increase in cerebral blood flow of the cortex from 30 min to 24 h when using laser Doppler flowmetry. The amount of lactate and the lactate/pyruvate ratio decreased after 7 days using the microdialysis technique. So, taurine can be credited with the decrease in the expression of certain cytokines and reduced cerebral edema. Taurine has an anti-inflammatory effect as it is converted into taurine chloramine, which inhibits the production of cytokines by downregulating their production following TBI. Carried out on rat models, the sham treatment showed 0.4% decrease, TBI and saline treatment showed 0.1% decrease, whereas taurine treatment showed 1.2% decrease in brain water content over 7 days.[16,47] The chemical structure is provided in **Figure 12**a. Dosage size was 200 mg day^{-1} kg^{-1} body weight. Fluid percussion injury was used as the TBI model.

8.2. Chloroquine

The antimalarial drug chloroquine (CQ) has been identified to offer neuroprotection following TBI by attenuating cerebral edema.[86] CQ suppressed neuronal autophagy and reduced the expression of certain cytokines to improve neurological functioning.[86] Upon the induction of trauma, a significant increase in the brain water content is seen. Alongside a decrease in brain water content, the motor function recovery is also

© 2021 The Authors. Advanced NanoBiomed Research published by Wiley-VCH GmbH

26999307, 2021, 11, Downloaded from https://advanced.onlinelibrary.wiley.com/doi/10.1002/anbr.202100001 by Koc University, Wiley Online Library on [05/09/2026]. See the Terms and Conditions (https://onlinelibrary.wiley.com/terms-and-conditions) on Wiley Online Library for rules of use; OA articles are governed by the applicable Creative Commons License

Table 8. The extent of implementation, advantages, and disadvantages of up-and-coming technologies in managing cerebral edema.

Device[a)]	Extent of implementation/ Purpose	Advantages	Drawbacks	References
VEPS	Prehuman trials/diagnosis	Inexpensive Noninvasive Can distinguish cerebral conditions	Limited human trials Accuracy declines with patient age Frequencies not fully characterized	[79]
OTD	Animal model/therapy	Optimum brain hydration Rapid decrease in edema Successfully implemented in mice models	Invasive technique Requires craniectomy Prone to infections and complications Lacks human trials	[80]
CoaxP	Cadavers/diagnosis	Accurate if placed correctly Nondestructive (reflection mode) Rapid scans last 20 s	Lack of in vivo data Yields an underestimate as poor contact due to bubble formation A high degree of uncertainty Unsuitable transmission in vivo	[81]
CopP	Cadavers/diagnosis	Better than CoaxP—immune to variable pressure Indicates extent of edema Rapid analysis	A high degree of uncertainty Sterilization issues Biocompatibility issues Noncontinuous monitoring	[82]
PMBS	Phantom model/diagnosis	Low cost Low-power tool Continuous edema monitoring Monitor edema shifts	Lack of in vivo data Hard to distinguish small shifts in peaks Sensitive to movement and orientation	[83]
EIT	In human trials/diagnosis	Noninvasive Successful animal trials Real-time monitoring Independent of operator experience	Contact with the scalp–scalp impedance Requires adjoining chemical treatments Sensitive to patient movement Nonuniform spatial resolution	[12]

[a)]EIT = electrical impedance tomography, VEPS = volumetric electromagnetic phase shift spectroscopy, CoaxP = coaxial probe for fast scanning of edema, CopP = coplanar probe for fast scanning of cerebral edema, PMS = portable microwave based systems, HFHD = hollow-fiber hydrogel device.

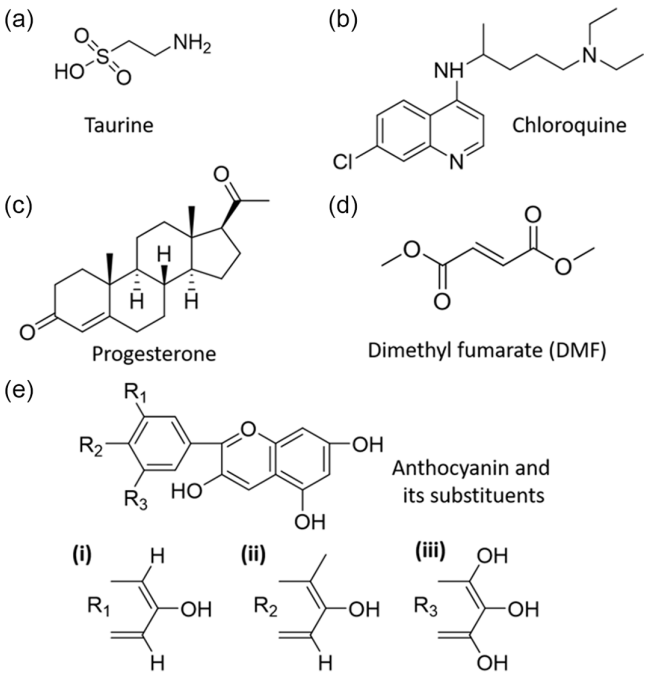


Figure 12. IUPAC structures of common compounds with the potential to be used as neuroprotectants: a) taurine, b) chloroquine, c) progesterone, d) DMF, e) anthocyanin with the three substituents as (i). (ii), and (iii).

observed between 24 h and 14 days. While TBI caused a spatial learning deficit, CQ significantly reduced the escape latency compared with the TBI + saline group.

Chloroquine offers neuroprotection by suppressing the neuronal autophagy. This has an action of preventing water build-up in the brain. Conducted on rat models, TBI + saline treatment (vehicle) showed an increase of 2.7% of brain water content after the first day due to the occurrence of edema but showed a decrease of 0.3% on the third day from day 12. Likewise, a 0.7% increase in brain water content is seen, however, from a much lower initial brain water content of 76.5%. On the third day, a 1.3% decrease in brain water content is seen from day 2.[86] The chemical structure is provided by Figure 12b. The dosage size was 3 mg day^{-1} kg^{-1} body weight. A weight-drop model was used as the TBI model.

8.3. Progesterone

Hypoxia–ischemia (HI)-induced brain damage leads to cerebral edema in its most basic forms. Aquaporin-4, which is a membrane protein, contributes to cerebral edema and leads to the accumulation of water in the brain tissue. Progesterone is a natural progestin, but its effects are not limited to reproduction as it has an impact on the central nervous system when secreted. Progesterone attenuates cerebral edema in rat models by inhibiting the expression of matrix metalloproteinase-9 and

© 2021 The Authors. Advanced NanoBiomed Research published by Wiley-VCH GmbH

26999307, 2021, 11, Downloaded from https://advanced.onlinelibrary.wiley.com/doi/10.1002/anbr.202100001 by Koc University, Wiley Online Library on [05/09/2026]. See the Terms and Conditions (https://onlinelibrary.wiley.com/terms-and-conditions) on Wiley Online Library for rules of use; OA articles are governed by the applicable Creative Commons License

aquaporin-4. Ultimately, progesterone reduces BBB damage and inhibits MMP-9 regeneration to protect the rat brains from the effects of HI. Progesterone attenuates cerebral edema in rat models by inhibiting the expression of matrix metalloproteinase-9 and aquaporin-4.[11] The chemical structure is provided in Figure 12c. The dosage size was 8 mg day^{-1} kg^{-1} body weight. No TBI model was used; rather it was based on HI as the rats were exposed to anoxic conditions for 2.5 h at 8% O_2 and 92% N_2 in a hermetic container.

8.4. Dimethyl Fumarate (DMF)

DMF is shown to attenuate cerebral edema formation by protecting the BBB integrity. DMF is an antioxidant which finds clinical applications in psoriasis and multiple sclerosis and has been shown to significantly prevent edema formation in vivo as rat stroke models were used. DMF prevented the disruption of inter-endothelial tight junctions and gap formation to stabilize the BBB. The protection of the BBB was due to increased Nrf2 activity. It also decreased the matrix metalloproteinase activity in the brain tissue. In vitro studies had previously confirmed its effectiveness as DMF and its primary metabolite monomethyl fumarate (MMF) as they were shown to increase the survival rate of astrocytes and neurons exposed to oxidative stressors, and it also attenuated the proinflammatory mediators in lipopolysaccharide (LPS)-activated microglia and astrocytes. Six mice in the DMF group were pretreated with DMF twice a day for three consecutive days before inducing experimental stroke, which reduced edema. The difference in the infarct volumes was not significant within 4 h; however, by the end of the day, significant differences could be seen.[87] DMF is shown to protect the BBB integrity as it attenuates the production of proinflammatory markers.[87] A 63% reduction in edema size (from 21.8 to 8.03 mm^3) was determined after 24 h of DMF administration at the rate of 15 mg kg^{-1}. The chemical structure is provided in Figure 12d. The dosage size was DMF dissolved in (DMSO) 26.8 mg ml^{-1} and diluted in phosphate buffer solution (PBS) to yield 1.875 mg ml^{-1}; administered intraperitoneally. No TBI model was used; instead the middle cerebral artery was occluded using a monofilament to induce focal cerebral ischemia.

8.5. Anthocyanin

Anthocyanin is an active ingredient found in the fruit of *Lyceum barbarum*, which is a traditional Chinese herb with vital biological activity. It has been shown to prevent cancer and age-related macular degeneration (AMD).[88] The extract protects the brain from BBB disruption and cerebral edema. Mice were subjected to a 2 h long middle cerebral artery occlusion (MCAO). The mice were segregated into two groups—namely, the vehicle (only PBS was administered) and the *L. barbarum* polysaccharide (LBP) group (with a dosage of 1 or 10 mg kg^{-1}). LBP extracts were prepared from the dried fruit of *L. barbarum*.

LBP treatment was shown to significantly improve the underlying neurological deficits as well as decreasing the infarct size and water content of cerebral edema. The brain was protected against BBB disruption, aquaporin-4 upregulation, and glial activation and it can be seen as a prophylactic neuroprotectant in cerebral edema.

The *L. barbarum* extract protects the brain from BBB disruption and cerebral edema.[84] The chemical structure is provided in Figure 12e and the substituents are represented by (i), (ii), and (iii). Two concentrations were tested: 1 and 10 mg kg^{-1}. No TBI model was used; instead the middle cerebral artery was occluded using a monofilament to induce focal cerebral ischemia.

8.6. Comparing the Efficacy of Neuroprotective Therapeutic Agents

Making an effective comparison based on the efficacy of the results is a difficult task as different concentrations of drugs were administered, different species of laboratory rodents were used, results were gathered at a different times, and there is an obvious inherent lack of data. However, the results given by **Figure 13** show visually the effectiveness of each of these treatments.

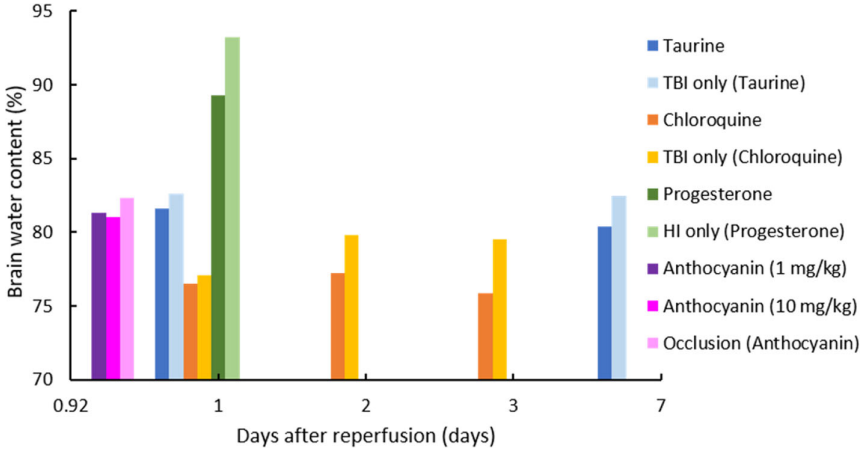


Figure 13. Comparison of the brain water content based on neuroprotective data. Data provided by Yang et al.,[84] Wang et al.,[11,16] Su et al.,[47] and Kunze et al.[87]

© 2021 The Authors. Advanced NanoBiomed Research published by Wiley-VCH GmbH

26999307, 2021, 11, Downloaded from https://advanced.onlinelibrary.wiley.com/doi/10.1002/anbr.202100001 by Koc University, Wiley Online Library on [05/09/2026]. See the Terms and Conditions (https://onlinelibrary.wiley.com/terms-and-conditions) on Wiley Online Library for rules of use; OA articles are governed by the applicable Creative Commons License

9. Patent Review of Neurodiagnostic Devices

Patents provide a useful insight into the technology that is due to be commercialized. This section looks exclusively at the device patents that are intended to monitor, and in some cases treat, cerebral edema. The patent literature was acquired using Google Patents and Lens in the last 10 years. The search criteria were based on the keyword "cerebral edema."

The AI-based patent search Dolcera was used to acquire patent publication data and it yielded 55 493 patents filed globally from 1996 to date. Of these, 29 171 (52.6%) are active patents and the rest are inactive. The application year, publication year, and priority year are plotted against the Gregorian year. Priority year indicates the time where the inventor can make an initial "priority" application, which allows the inventor to file additional patents in other countries within 12 months. It also allows the inventor to obtain additional experimental data to support the patent application as well as to critically assess the commerciality of the invention. **Figure 14** shows the numbers of patents filed and published as well as the number of priority applications. The year 2008 marked the highest number of patent applications, but these were not recovered since; however, they have remained steady thereafter.

9.1. Patented Devices in Managing Cerebral Edema

This section describes the patents that have been invented as a means of detecting and managing cerebral edema. **Table 9** provides a succinct summary of all the six patents that are elaborated on in this section.

9.1.1. Surface Dialysis and Cooling Probe

This device operates on the principle of osmotic removal of water using chemical agents such as mannitol.[89] However, the major drawback of using neuroprotective agents like mannitol is that the osmotic agents can come in direct contact with damaged brain tissue and can aggravate the swelling.[90] This is known as the rebound phenomenon.[91] This requires a craniectomy to allow outward swelling of the brain.

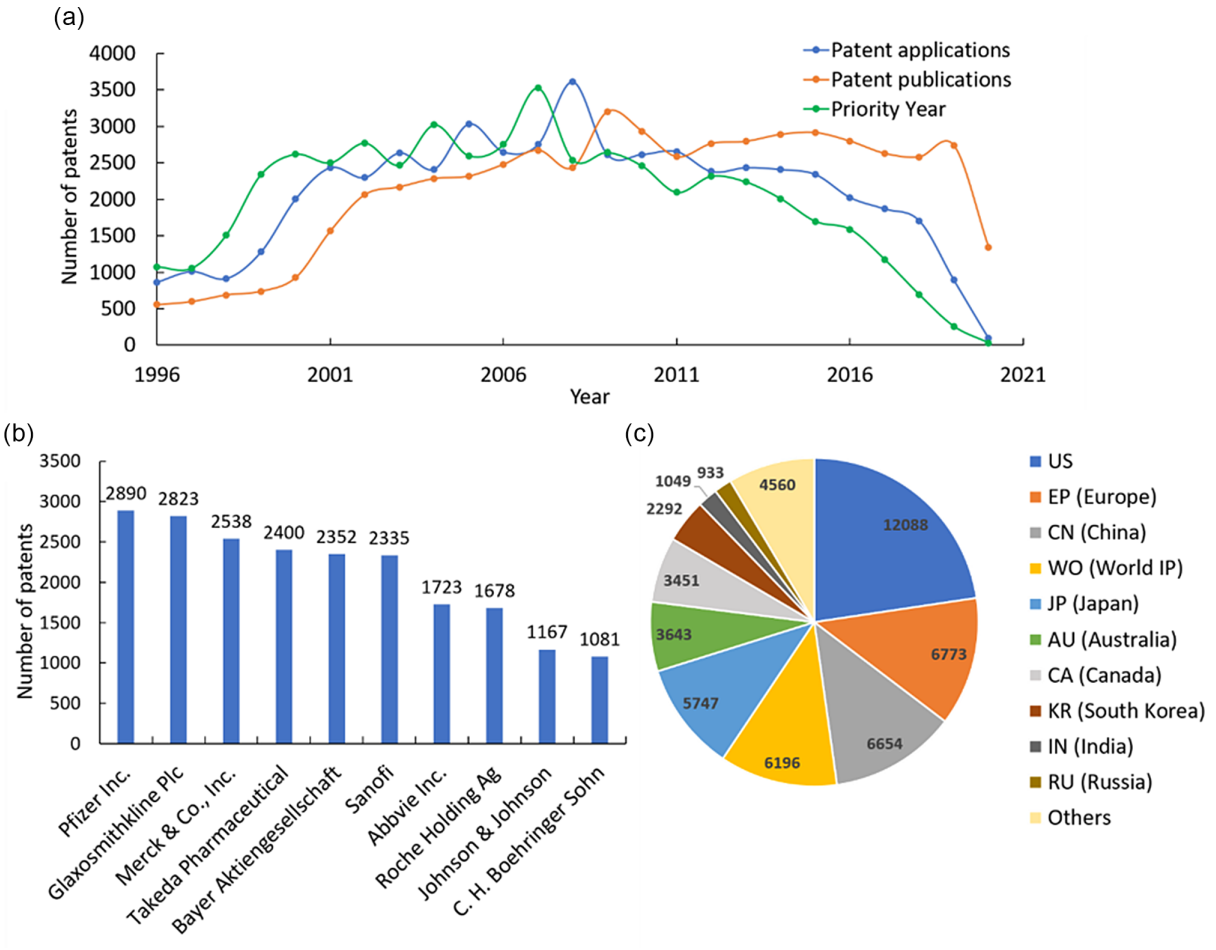


Figure 14. Statistical information concerning cerebral edema patents. a) The number of patent applications, (patent) publications, and priority years based on data compiled by Dolcera based on the keyword "cerebral edema." b) Top ten corporate owners of cerebral edema patents till date. c) The number of patents filed by country. The United States has the highest number of patents, with 22.6% of all patents filed till date. Data obtained from Dolcera.

© 2021 The Authors. Advanced NanoBiomed Research published by Wiley-VCH GmbH

26999307, 2021, 11, Downloaded from https://advanced.onlinelibrary.wiley.com/doi/10.1002/anbr.202100001 by Koc University, Wiley Online Library on [05/09/2026]. See the Terms and Conditions (https://onlinelibrary.wiley.com/terms-and-conditions) on Wiley Online Library for rules of use; OA articles are governed by the applicable Creative Commons License

Table 9. Summary of the patents discussed and the nature of monitoring.

Device and principle of operation	Working principle/purpose	Patent number	Publication year	Inventor
Surface dialysis and cooling	Invasive/therapy	US8012116B2	2011	[90]
Thermal conductivity and diffusivity	Invasive/diagnosis–monitoring	US20140303513A1	2014	[6]
Electromagnetic wave propagation properties	Noninvasive/diagnosis	US9456757B1	2016	[92]
Magnetic induction phase shift spectroscopy	Noninvasive/diagnosis	AU2019257529A1	2019	[93]
Focal cooling to the brain and spinal cord	Invasive/therapy	US2020/0188646A1	2020	[5]

This device was tested in a rat model to reduce brain swelling using a semipermeable membrane. **Figure 15**a shows the device in principle, while (c) and (d) show its implementation and the device probe schematic. The cryoinjuries were induced by exposing the rats to a copper rod dipped in liquid nitrogen, which created a necrotic lesion with vasogenic edema, and thereafter, dialysis was performed for 2 h. The device was fastened in place using sutures or pressure from the scalp. The precooled dialysate (dialysis solution) has a greater osmolarity than that of the brain fluid and contains 15% of the mixture of dextran, inulin, and hydroxyethyl starch. The dialysate solution is flowed through the inlet port into the inner chamber past the semipermeable membrane and out of the inner chamber through the outlet port. Cellobiose, a naturally occurring plant saccharide, constitutes the dialysis membrane, whereas the PMMA constitutes the semipermeable membrane. The warm interstitial fluid flows osmotically into the inner chamber of the body through the semipermeable and dialysis membranes, where it is subsequently removed.[90]

The molecular size of dextran and other species in the dialysate solution is greater than the pore size of the dialysis membrane and is thus prevented from contacting the brain. The permeability of the hemodialysis membrane is measured using the ultrafiltration coefficient (K_{UF} [ml hr^{-1} mmHg^{-1}]) and is thinner than 50 µm to ensure flexibility. This procedure avoids needles, so it is less invasive and prevents further brain damage. A decrease in the spread of water content in the rat brain was tested using Evans blue. It was found that the volume of Evans blue in millimeter cubed required for the sham surgery case was 36.8 ± 2.1 mm^3, whereas for the dialysis this value

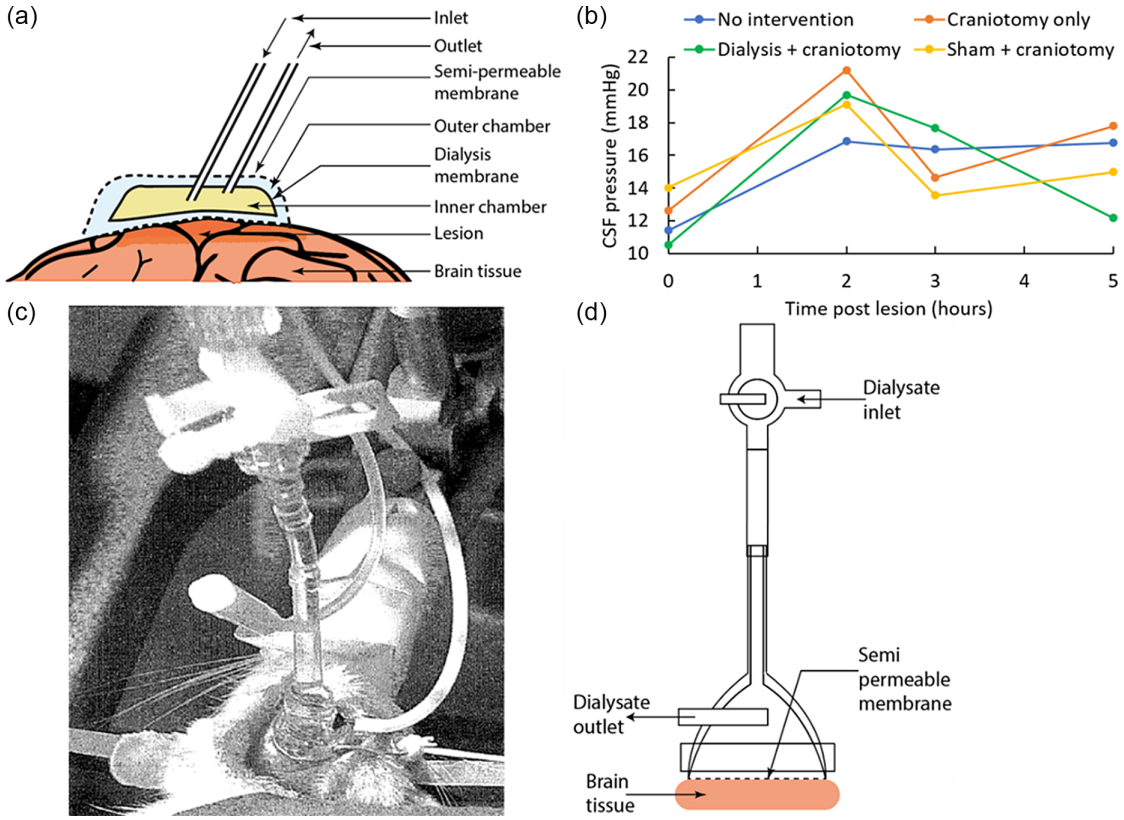


Figure 15. Surface dialysis and cooling probe used in the management of cerebral edema. a) Experimental osmotic flow cell. b) Testing the efficacy of the surface dialysis probe. c) Probe used in animal models. Reproduced with permission.[90] Copyright 2011, US Patent. d) Cutaway section of the osmotic dialysis probe for use in human beings, which can be placed atop brains after craniectomy.

© 2021 The Authors. Advanced NanoBiomed Research published by Wiley-VCH GmbH

26999307, 2021, 11, Downloaded from https://advanced.onlinelibrary.wiley.com/doi/10.1002/anbr.202100001 by Koc University, Wiley Online Library on [05/09/2026]. See the Terms and Conditions (https://onlinelibrary.wiley.com/terms-and-conditions) on Wiley Online Library for rules of use; OA articles are governed by the applicable Creative Commons License

26999307, 2021, 11, Downloaded from https://advanced.onlinelibrary.wiley.com/doi/10.1002/anbr.202100001 by Koc University, Wiley Online Library on [05/09/2026]. See the Terms and Conditions (https://onlinelibrary.wiley.com/terms-and-conditions) on Wiley Online Library for rules of use; OA articles are governed by the applicable Creative Commons License

was lowered to $19.9 \pm 3.3\,\mathrm{mm}^3$. This shows that the spread of edema was curtailed by the means of this device. In sham dialysis, the fluid migration is inward, but the converse is true when the device is used. The larger area of the contact and the greater volume allows greater and faster removal of water, respectively.[90]

Local cooling of the brain to 32 °C is shown to provide a beneficial influence on the underlying physiology. This was achieved by precooling the inlet fluid in an ice bath and the results are reflected in Figure 15b. However, the inventor acknowledges that this is difficult to achieve. Each of the 20 rats in the study was distributed equally into four groups ($n = 5$), where each group received a TBI injury. These include no intervention, decompressive craniectomy (DC) only, DC and sham dialysis, and DC and dialysis. Figure 15b shows the results. The CSF pressure remained steady after day two, which shows the presence of edema. Although the device causes additional pressure elevation at day 2, the CSF pressure is restored close to the prenormal levels, which proves the efficacy of the device.

Compared to the probe used for the rat model, the device would need to be adapted for applications in humans by scaling up the dimensions. The devices are expected to perform better for localized edema and are not limited to those cerebral in origin, such as tissues and muscles.[90]

9.1.2. Real-Time Edema Monitor Using Thermal Measurements

This device provides real-time edema monitoring capabilities at the point of care through patient-specific tissue conductivity and tissue perfusion pressure that is assisted by the empirically developed perfusion coefficient of thermal conductivity. It is used to distinguish tissue intravascular and extravascular water (edema) contributions.[6]

This probe allows seamless coupling with the ICP probes. It allows quantitative tracking of the therapeutic interventions. The probe can determine the thermal response of the tissue by applying thermal energy and determine the water content as a function of thermal energy or power. It works on the principle that as the water content in the brain increases, the thermal conductivity and diffusivity also increase, which are measurable. Dual-set thermistors are embedded in the minimally invasive thermal probe, which can convert the in vivo thermal data into electrical signals. A narrow-gauge catheter is used for this purpose, and its tip is 1 mm in diameter, thus rendering it minimally invasive. This is electrically communicated with a data processor. A schematic of the device is shown using **Figure 16**a.

The proximal thermistor is used to monitor the tissue baseline temperature and accounts for any temperature fluctuations. The second distal thermistor heats the surrounding tissue slightly (≈2 °C) at intervals above the tissue temperature baseline using a power source. The power dissipated is typically 5–10 mW. The heat-carrying capacity through conduction of tissue or convection of the blood flow is determined. Any deviations from the intrinsic value are determined and the value of convective heat transfer is disregarded. The conductivity value is correlated with the amount of water present. The thermal physics in the tissue is modeled using the bioheat equation given by Equation (5).

The bioheat equation to determine the tissue thermal conductivity, K, is shown subsequently.

The equation is based on ρ (tissue density), c (tissue specific heat), T (temperature rise in tissues), ω (tissue perfusion), ρ_b (blood density), and c_b (blood specific heat).

$$\rho c \frac{\partial T}{\partial t} = K\nabla^2 - \omega \rho_\mathrm{b} c_\mathrm{b} T \tag{5}$$

The direct determination of the conductivity value may produce erroneous results due to some margin of error. Consequently, an iterative process is used to accurately optimize the water content. This is achieved by conducting several heating cycles and at separate times, where the temperature is elevated and allowed to cool to the baseline temperatures. A second cycle is used to obtain a more accurate value using the prior perfusion value as in each case the convective value is disregarded. This allows the conductivity value to converge to a more accurate value. This is achieved by the monitor software, which separates the conductive and convective contributions.

This probe is correlated with historic biopsy edema data and is accurate within 2%. In comparison with the Hemedex probe, the accuracy of the conductivity value has been estimated to be within 1%. This shows the accuracy of the probe in monitoring cerebral edema.[6] Figure 16b shows the plot of thermal conductivity against perfusion time.[6]

9.1.3. Electromagnetic Wave Propagation Properties for Edema Monitoring

This invention presents a continuous, noninvasive means of monitoring cerebral edema using the electromagnetic wave propagation properties at the point of care. The underlying pathophysiology has the impact of altering the properties of interest. These properties include the tissue permittivity, which determines the wave propagation velocity. This method does not rely on conductivity measurements, so the readings obtained are accurate as the method disregards the skin and electrode conductive properties.[92]

CSF can be distinguished easily as it has a lower dielectric constant than the brain tissue. However, blood has a higher dielectric constant compared to brain tissue and hence allows differentiation among hydrocephalus, intracranial hemorrhage, and cerebral edema. The dielectric constant determines the wave propagation speed.[92]

The relative attenuation coefficient (RAC) is defined to quantify the EM wave propagation through the brain tissue with different conductivities and dielectrics, which is given by Equation (6).[92]

The relative attenuation coefficient (RAC) used for the EM wave propagation is obtained as follows

$$\mathrm{RAC} = \frac{1}{r\omega} \ln\left(\frac{|E_1|}{|E_2|}\right) = \frac{1}{\omega}\left(k_{l,2} - k_{l,1}\right) \tag{6}$$

where $k_{l,1}$ is the imaginary part of the complex wavenumber k_1, which is the baseline of conductivities and dielectric constants measured early. $k_{l,2}$ is the imaginary part of the complex wavenumber k_2. ω is the angular frequency of the EM wave, and E_1

© 2021 The Authors. Advanced NanoBiomed Research published by Wiley-VCH GmbH

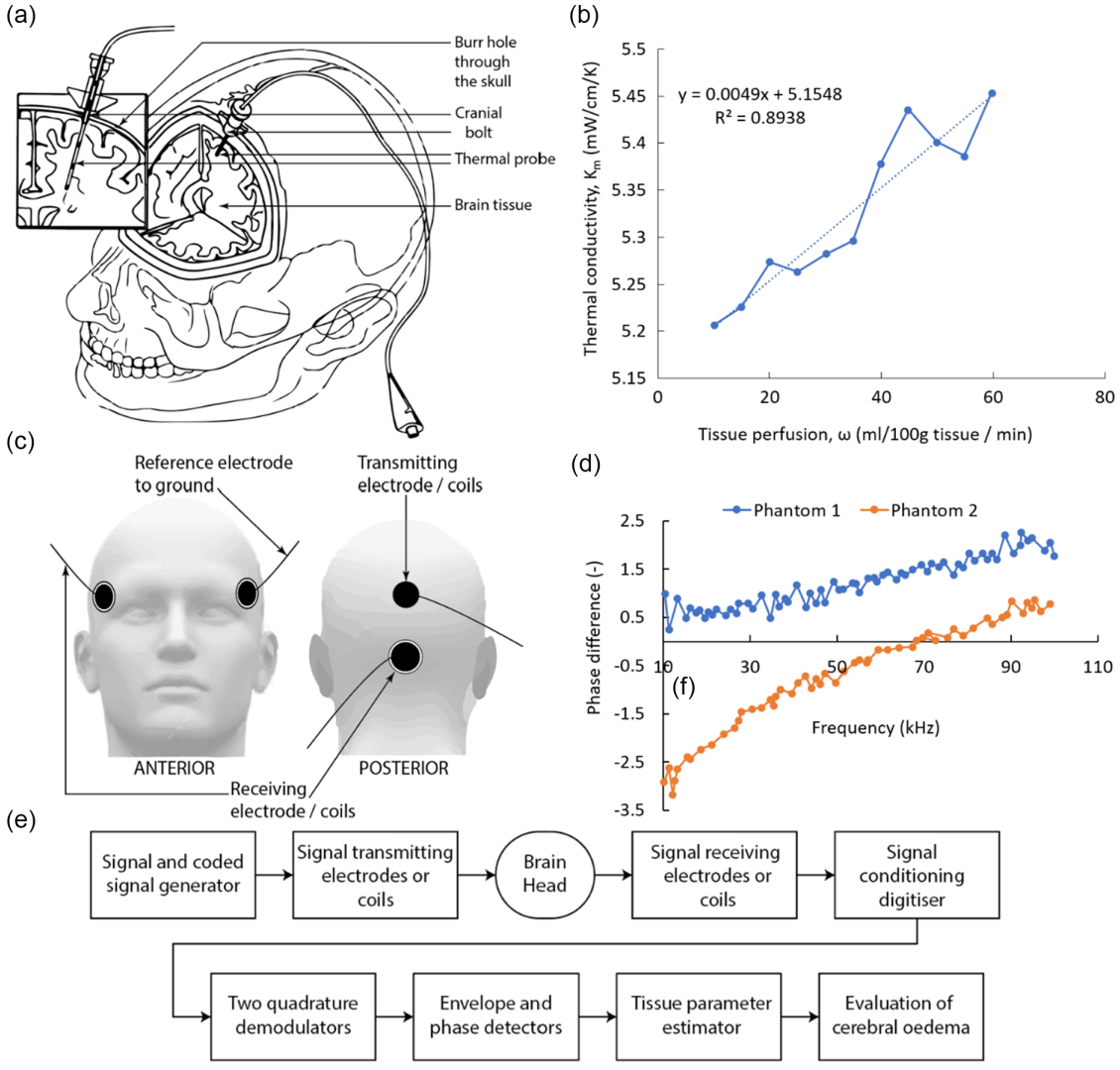


Figure 16. The device implementing thermal conductivity and wave propagation properties to determine cerebral edema. a) Thermal measurement probe used in vivo. Adapted with permission.[6] Copyright 2014, US Patent. b) Plot of thermal conductivity against tissue perfusion. c) The transmitting and receiving electrodes placed on the anterior and posterior of the head. d) Plot of the phase difference against frequency. Reproduced with permission.[92] Copyright 2016, US Patent. e) Flowchart to demonstrate the process used to determine the phase shift and its correlation with cerebral edema.

and E_2 are the electric field strength. The RAC is determined by comparing the attenuation of the EM propagation through brain tissue to a baseline.[92]

The device consists of an electrode source that generates electromagnetic radiation at the electrodes or coils. The continuous and monochromatic signals, as well as broadband pulses with multiple frequencies, are propagated through the brain from the transmitting electrodes. The sensors beside the transmitter as well as on the other side of the head (for the case of two receiving electrodes) receive the propagated wave. The receivers can be placed anywhere on the head, and different configuration allows for the measurement of pertinent parameters such as RAC. The electrodes can be fastened using a headband or even surgical tape. The received signal is conditioned, amplified, filtered, and converted into a digital signal using the signal-conditioning digitizer. The quadrature detectors determine the magnitude and phases of the said wave and a parameter estimator. It also determines a range of quantifiable parameters, which facilitate the increase in sensitivity and specificity of monitoring status.[92]

Compared to the MIPS device (200 MHz), this device operates at a lower frequency in the range 10–100 kHz. Although the device has been successfully demonstrated within this range of frequencies, the inventors hypothesize that the device should be functional for higher and lower ranges of frequencies.[92]

Phantoms, which were made using pig skin powder, were used to test the efficacy of this device. The amount of water was varied to represent a different amount of edema. Some notable benefits of this device include continuous and point-of-care diagnostic capabilities, as well as low cost, ease –of use, and an automated interface, which requires minimal intervention.[92] Figure 16c shows the transmitting and receiving electrodes placed on the anterior and posterior of the head, (d) shows

© 2021 The Authors. Advanced NanoBiomed Research published by Wiley-VCH GmbH

26999307, 2021, 11, Downloaded from https://advanced.onlinelibrary.wiley.com/doi/10.1002/anbr.202100001 by Koc University, Wiley Online Library on [05/09/2026]. See the Terms and Conditions (https://onlinelibrary.wiley.com/terms-and-conditions) on Wiley Online Library for rules of use; OA articles are governed by the applicable Creative Commons License

the plot of the phase difference against frequency,[92] and (e) shows a flowchart to demonstrate the process used to determine the phase shift and its correlation with cerebral edema.

9.1.4. Magnetic Induction Phase Shift Spectroscopy for Tracking Fluid Changes

This technique is a noninvasive means of detecting fluid changes caused by cerebral edema. The underlying principle is the magnetic induction phase shift spectroscopy (MIPS). The device consists of a housing that contains a processor, a transmitter located on one side of the head, and a receiver, which is located on the other side of the head. The transmitter converts a time-varying current into a time-varying magnetic field at a range of fundamental frequencies, which pass through the head. The detector on the other side of the head detects the time-varying magnetic field. This is converted into a time-varying current. Although the frequency remains unaltered, there is a change in the phase, which is measured and is correlated with the water content in the brain. The phase shift or magnitude change is caused by the internal cerebral anatomy, and this is compared against the phase shift or magnitude change caused by another time-varying magnetic field. Equation (7) is used to determine the phase shift using the angles of interest, $n_{t,}$ and offset. The frequency signal is processed using the fast Fourier transform.[93]

The phase shift equation using the angle of interest and offset is shown as follows

$$\text{Phase shift} = 90° + \frac{n_{\text{offset}}}{n_{\text{t}}} + 360° \tag{7}$$

The relative permittivity of body fluids is higher than most tissues, so it has a greater bearing on the overall electromagnetic phase shift in the brain. The MIPS technique was previously shown as a promising technique, yet its mass production was somewhat limited, which encouraged the development of this device.[93]

Radiofrequency, i.e., frequencies below 200 MHz, were used for this purpose and the phase shift is a function of the loss factor. At this frequency, the EM waves are not fully formed as the wavelength of the radio waves (1.5 m) is greater than the head width and is said to be in the near field. In this region, the loss factor dominates, which is dependent on the ionic content of the brain fluid. This enables the subclassification of the fluid compositions. Detecting the fluid level changes can dictate the treatment methods for the effective treatment of the underlying condition. Magnitude changes, as opposed to phase shifts, are used to measure the change in electrical properties of tissues.[93]

Some of the notable advantages of this device are the improved performance, usability, and manufacturability of the device components. **Figure 17**a shows the circuit diagram of the system, which can detect a phase shift, and Figure 17b shows an exploded view of the proposed MIPS device.[93] Abnormal fluid changes will dictate treatment methods for abnormal conditions. The invention reports an improvement in the accuracy and repeatability of the phase shift measurements. Figure 17c shows the evolution of the parenchyma temperature against time for varying distances from the parenchyma and (d) shows the evolution of the catheter inlet and outlet pressure over time.

9.1.5. Focal Cooling to the Brain and Spinal Cord

In traumatic brain injuries, there is a link between temperature elevation and increased intracranial pressure. Hence, the management of cerebral edema through cooling is provided as an alternative to conventional management techniques. It has been demonstrated that hypothermic treatment offers neuroprotection against cerebral edema. The focused cooling suppresses the formation of free radicals, inflammation, and metabolic demands. Although lumbar drainage has been used for over a decade to treat thoracic and thoracoabdominal aortic aneurysms, its utility in treating cerebral edema is just being realized.[5]

Typical temperatures in hypothermic treatment include 32–34 °C. However, current hypothermic techniques present a whole host of challenges, including arrhythmias, infection, sepsis, coagulopathy, and electrolyte abnormalities. This presents an opportunity to introduce this patent that would not pose the same risks as the current techniques. For example, the components used in the device may be simple to facilitate decontamination, and the catheters and other components such as sealants may be coated with protein or microorganism repellent coatings, or antibiotic coatings, such as silver nanoparticles.[5]

These embodiments make use of a multilumen (multiple inlets) catheter, and the CSF may be withdrawn, cooled, and returned through the outlet lumen of the catheter. In certain embodiments, the CSF can be extracted from the caudal end of the spine, while in others, it can be extracted from the ventricles in the brain after a craniectomy; there may be minimal or no difference between the catheters used in either location. Figure 17c,d shows embodiments of cross-sections of double- and triple-lumen probes that can be inserted through a single access port. In the case of double-lumen probes, the temperature of the CSF is determined extracorporeally; however, it cannot necessarily determine the in vivo temperature. The catheters can be coiled helically and placed inside a stylet to allow for a greater surface area of heat transfer. Stylets can be used to provide additional structural rigidity to the catheters. Alternatively, a heat transfer fluid such as saline or perfluorocarbons may be circulated through the cooling lumen of the catheter. Sensors can be mounted on the catheters to measures the properties of the target site and dictate the consequent treatment. They may also help to characterize the extracted fluids. Additionally, EEG electrodes may be affixed on the catheters to acquire EEG data. The catheter tubing may be designed in a shape that discourages blockages. Tubing occlusions may be detected by monitoring deviations from expected flow rates.[5]

The current method is tested for bovine and human subjects. The device can be used to modulate the flow of the circulating CSF. Cooling to and maintaining at 31 °C has an effect of decreasing the metabolic rate, which contributes to an improved patient outcome. In severe manifestations, the temperature could be lowered to 25 °C, which would cause a decline in the cytotoxic load by up to 50%.[5] The process can be automated

© 2021 The Authors. Advanced NanoBiomed Research published by Wiley-VCH GmbH

26999307, 2021, 11, Downloaded from https://advanced.onlinelibrary.wiley.com/doi/10.1002/anbr.202100001 by Koc University, Wiley Online Library on [05/09/2026]. See the Terms and Conditions (https://onlinelibrary.wiley.com/terms-and-conditions) on Wiley Online Library for rules of use; OA articles are governed by the applicable Creative Commons License

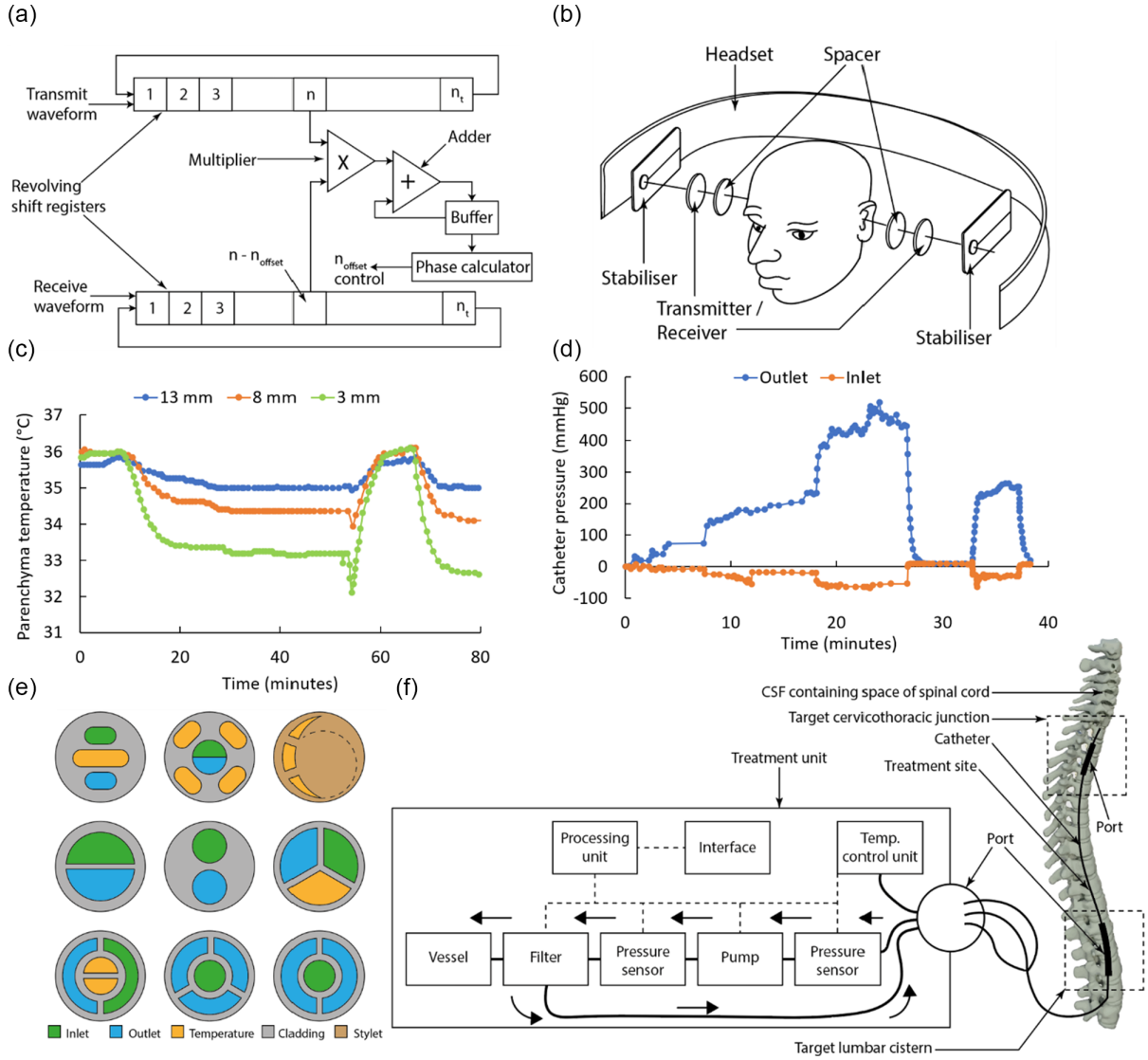


Figure 17. Devices used for magnetic induction phase shift spectroscopy and to provide focal cooling to the brain and spinal cord. a) Circuit diagram of the patented MIPS device. b) Exploded view of the proposed MIPS device. The schematic shows one of the many embodiments patented by the inventor. Reproduced with permission.[93] Copyright 2019, US Patent. c) Evolution of parenchyma temperature against time for varying distances from the parenchyma. d) Evolution of catheter inlet and outlet pressure over time. e) Cross-sections of the catheters used in the extraction and treatment of CSF. Reproduced with permission.[5] Copyright 2020, US Patent. f) Schematic of the focal cooling probe.

by implementing a feedback control system and advanced sensors to monitor and maintain a neuroprotective state, which requires minimal human intervention. The body produces around 400–500 mL of CSF per day, and the device can be configured to treat 120–1800 mL of CSF per hour in certain embodiments. At the normal body temperature, the maximum load is 800 mL per hour. Significant costs can be saved using gravity-based CSF drainage systems. Cooling algorithms can be coded into the system, which can impart hypothermic treatments to the patients that can adapt to the dynamics of edema. Certain types of ultra or microfilters may be implemented to separate cytokines and other proteins for further analysis. A peristaltic pump may be used, which may reduce the sterilization of complex pump components.[5]

10. Opportunities and Challenges of Current Techniques

Diagnosis and management of cerebral edema can be achieved through invasive and/or noninvasive methods, assisting clinicians to find optimum therapeutic interventions. Although a ventriculostomy catheter is an accurate gold standard for invasive neuromonitoring with the ability to measure global ICP, the difficulty of placement, risk of infection and hemorrhage, and inability to drain CSF and monitor ICP concomitantly are major challenges of this method. Alternative neuromonitoring techniques (e.g., intraparenchymal monitors, subdural catheters, and epidural catheters) are less invasive (compared to ventriculostomy catheters) with easier placement and fewer risks of

© 2021 The Authors. Advanced NanoBiomed Research published by Wiley-VCH GmbH

26999307, 2021, 11, Downloaded from https://advanced.onlinelibrary.wiley.com/doi/10.1002/anbr.202100001 by Koc University, Wiley Online Library on [05/09/2026]. See the Terms and Conditions (https://onlinelibrary.wiley.com/terms-and-conditions) on Wiley Online Library for rules of use; OA articles are governed by the applicable Creative Commons License

26999307, 2021, 11, Downloaded from https://advanced.onlinelibrary.wiley.com/doi/10.1002/anbr.202100001 by Koc University, Wiley Online Library on [05/09/2026]. See the Terms and Conditions (https://onlinelibrary.wiley.com/terms-and-conditions) on Wiley Online Library for rules of use; OA articles are governed by the applicable Creative Commons License

complication. However, while the intraparenchymal monitor cannot be calibrated in vivo and damage of fiber optics is conceivable, the other two alternative methods are less accurate and reliable. Considering noninvasive methods, no approach has been reported to detect fluid changes and edema extent accurately and continuously.[34,39,42]

CT and MRI are widely used techniques for cerebral edema imaging. Although NECT is a relatively insensitive method, it is the first-line imaging modality due to being easy to obtain and the ability to exclude life-threatening cases. The use of CECT, as an alternative to conventional MRI, can enhance the results of NECT as it is more sensitive to noncontrast MRI, whereas CECT is less sensitive than CEMRI. Moreover, MRS enables spectroscopic differentiation of different biomarkers and distinguishing between edema and neoplasms. The main challenge faced by MRS is variable biomarker concentration ratios (i.e., thresholds are advisory). Despite being limited to 3D imaging, DWI adequately distinguishes between HI injury and focal infarction, which can be used as a tool for assessing the efficacy of neuroprotective agents. DTI allows detailed imaging in six directions, enabling early detection of brain edema during HI reperfusion. However, the ADC value varies and decreases with age.[10,60]

Following diagnosis, cerebral edema management technologies should be used. VEPS is a cost-effective and noninvasive method that can distinguish cerebral conditions. Nonetheless, its accuracy reduces for older patients, and frequencies are not fully characterized.[79] Although OTD was implemented in mice models, reporting a rapid decline in edema, it is an invasive method that requires craniectomy and can engender infection.[80] The use of CoaxP allows nondestructive and rapid scans (≈20 s) with accurate results (if placed correctly), whereas lack of in vivo data and bubble formation are the main challenges of CoaxP.[81] Despite the inability for continuous monitoring and having biocompatibility as well as sterilization issues, CopP is a rapid method to indicate the extent of edema better than CoaxP due to CopP's insusceptibility to variable pressure.[82] PMBS, as a low-cost method for continuous monitoring of edema and its shifts, suffers from a paucity of in vivo data, sensitivity to movement and orientation, and difficulty distinguishing shifts in peaks.[83] EIT is a noninvasive method for real-time monitoring of edema, which has yielded successful animal test results. However, nonuniform spatial resolution, sensitivity to movements of the patient, and requiring adjoining chemical treatments are major challenges of using EIT.[12]

11. Discussions and Future Directions

TBI is prone to misclassification due to an inherent lack of robust quantitative and qualitative modalities. Additionally, external factors can often interfere with the accurate classification, so a better means of determining the TBI severity is urgently needed.[18] Cerebral edema is often dichotomized into vasogenic and cytotoxic types.[12] However, for the effective diagnosis and treatment of the underlying pathology, further classification is imperative as this would dictate the effective treatment through impactful modalities. These biomolecular pathways are interrelated and our understanding of biomolecular mechanisms of edema formation is still in its infancy despite numerous studies.[13] Hence, additional research is necessary.

Active research on the development of continuous, point-of-care neuromonitoring is driven by the need for high functionality and noninvasiveness as well as significant ease of operation and miniaturization.[37] There is an inherent lack of clinical data, which causes a bottleneck in the clinical adoption and widespread implementation of neuromonitoring technologies.[51] A noteworthy example is that of SjvO2 monitoring, as its impacts on the outcomes of TBI have not been elucidated in random control trials.[52] Moreover, the implementation of TCD as a monitoring modality is somewhat limited due to lack of evidence in patients with severe TBI.[52] That said, additional research in this area is generating swatches of data, which hold the potential to accelerate the implementation of machine learning techniques to current devices in the future.

According to the Brain Trauma Foundation, ICP should be monitored in all salvageable patients with a severe TBI.[52] Despite the superior accuracy of ICP probes, they are often inadequate in diagnosing the onset of cerebral edema.[6,41] Additionally, the widespread implementation of noninvasive devices is restricted by the inaccuracies in the results obtained. This is particularly true in the case of noninvasive ICP measurements using TCD and CMD, which suffer from inaccuracies. Additionally, the NIR signal may be attenuated by the extracranial tissue; multioptode devices such as INVOS circumvent this problem using 2 detectors and a subtraction-based algorithm,[51] although active interest in this area is spurred by the downsides of invasive devices, including hemorrhage and infection.[78]

Despite the inclination of clinicians toward conventional technology such as MRI, there is a growing interest in the use of CMD. CMD can provide dynamic and real-time information as opposed to the static information provided by MRI.[57] Additionally, the point-of-care implementation of CMD is beneficial as critically-ill patients need to be transported back and forth for MRI scams.[57]

Animal models are widely used to give an in vivo assessment of TBI through several models such as rigid indentation, fluid percussion, impact acceleration, weight drop, and dynamic cortical deformation.[27,86] However, head injury is a spontaneous and unpredictable process and no single animal model can produce all the pathological conditions that are observed in humans. However, any mice not depicting TBI were excluded from further studies. It is important to note that no imaging modality is self-sufficient, and an enhanced knowledge can be acquired when more than one diagnostic tool is used in tandem. Additionally, the devices and neuroprotectants could be combined to yield better clinical outcomes; DWI has been used as a tool for assessing the outcome and effects of the neuroprotective agent.[64]

Currently, the brain monitoring market size is estimated to be US$ 6.3 billion by a market study conducted by Markets and Markets Research Private Ltd. This includes the current devices such as MRI, ICP monitors, and the vast array of invasive devices and their implementation in hospitals, clinics, and ambulatory service centers (ASC). This market is forecasted to reach US $8.6 billion at a compound annual growth rate of 6.2%. This highlights the market opportunity and the need for optimal

© 2021 The Authors. Advanced NanoBiomed Research published by Wiley-VCH GmbH

solutions in neuromonitoring. According to the 2019 market research data, North America accounted for the largest share of the brain monitoring market and is reflective of the number of patents published in the United States. However, the Asia Pacific is the fastest-growing region in the brain-monitoring market and significant future research is likely to be contributed by this region.[94]

The impact of COVID-19 highlighted the need for remote monitoring and patient engagement solutions. Many hospitals and healthcare facilities are trying to relocate and expand patient monitoring to bedside settings or other temporary setups as current hospital spaces are being used or reserved for critically ill COVID-19 patients. This also means that fewer ventilators and MRI, EEG, and other devices are available for elective neurology procedures. A tectonic shift in the research goals toward treating and managing COVID-19 would retard the progress in the field of neurodiagnosis for a few years, although progress in treating other conditions will inevitably contribute to change in neuromonitoring and neurocritical care. Additionally, there are additional costs associated with supply chains and logistics and the turbulence in this field is likely to extend into the next few quarters. In future studies, a greater emphasis must be placed on TBI-induced injuries as it accounted for the largest share of the brain monitoring market in 2019 that was driven by a surge in incidences across the globe.[94]

12. Conclusion

This review provided an overview of the current and upcoming approaches in the diagnosis and treatment of cerebral edema. Clinicians prefer the invasive devices due to their superior accuracy, which is spurring further development. However, there is a gradual shift toward the implementation of noninvasive devices due to their obvious advantages, including improved sterility and lack of invasiveness. That said, noninvasive devices suffer from inaccuracies and the lack of their commercialization proves that significant research is needed in this domain. There is an active research interest in bridging the gap between invasive and noninvasive devices as well as the implementation of multimodal approaches; the current research is directed toward unified semi-invasive procedures. This is reflected in the patents and the latest research outcomes from this field.

The inherent lack of a single diagnostic modality of cerebral edema necessitates the multimodality of neuromonitoring to obtain an enhanced understanding of the complex physiological processes. Additionally, to improve the effectiveness of the treatment modalities, it is recommended to combine chemical agents and neuromonitoring techniques for improved clinical outcomes. Although this is relatively easy to implement with invasive devices as chemical agents need a form of surgical administration, coupling them with noninvasive devices may refute the advantages of noninvasiveness.

Although global events such as COVID-19 may have faltered the research endeavor in TBI and cerebral edema, by the rising number of TBI patients and the obvious shortcomings of the current economy of devices, it is evident that research in these areas will accelerate in the years to come.

Acknowledgements

ToC image has been designed using resources from Flaticon.com. K.P.D. acknowledges Sam Davies, Chloe Sous, and Yuqian Zhang for providing advice and assistance with this project. S.T. acknowledges the Tubitak 2232 International Fellowship for the Outstanding Researchers Award (118C391), Alexander von Humboldt Research Fellowship for Experienced Researchers, Marie Skłodowska-Curie Individual Fellowship (101003361), and Royal Academy Newton-Katip Çelebi Transforming Systems Through Partnership award (120N019) for their partial financial support. Opinions, interpretations, conclusions, and recommendations are those of the authors and are not necessarily endorsed by the TÜBİTAK. N.J. acknowledges the Fundamental Research Funds for the Central Universities (YJ202152). The authors have no other relevant affiliations or financial involvement with any organization or entity with a financial interest in or financial conflict with the subject matter or materials discussed in the manuscript apart from those disclosed.

Conflict of Interest

The authors declare no conflict of interest.

Keywords

acquired brain injuries, biomarkers, cerebrospinal fluid, neuromonitoring, neurocritical

Received: January 1, 2021
Revised: June 20, 2021
Published online: August 16, 2021

[1] C. M. Miller, M. T. Torbey, *Neurocritical Care Monitoring*, Demos Medical Publishing, LLC, New York **2014**.
[2] J. Claassen, L. J. Hirsch, J. A. Frontera, A. Fernandez, M. Schmidt, G. Kapinos, J. Wittman, E. S. Connolly, R. G. Emerson, S. A. Mayer, *Neurocrit. Care*, **2006**, *4*, 103.
[3] S. Y. Ng, A. Y. W. Lee, *Front. Cell. Neurosci.* **2019**, *13*, 1.
[4] J. Badaut, J. H. Zhang, *J. Neurosci. Res.* **2018**, *98*, 19.
[5] A. Vase, D. W. E. Evans, Devices and methods for providing focal cooling to the brain and spinal cord, **2020**, https://patents.google.com/patent/US20200188646A1/en?oq=US+2020%2F0188646+A1.
[6] Bowman, H. F. (**2014**) Edema Monitor, https://lens.org/160-727-330-535-868.
[7] K. M. Busl, T. P. Bleck, P. N. Varelas, *JAMA Neurol.* **2019**, *76*, 612.
[8] F. Fu, B. Li, M. Dai, S.-J. Hu, X. Li, C.-H. Xu, B. Wang, B. Yang, M.-X. Tang, X.-Z. Dong, Z. Fei, X.-T. Shi, M. A. Deli, *PLoS ONE* **2014**, *9*, 113202.
[9] G. Li, K. Ma, J. Sun, G. Jin, M. Qin, H. Feng, *Sensors (Switzerland)* **2017**, *17*. 537.
[10] H. Wang, X. Wang, Q. Guo, *Pediatr. Radiol.* **2012**, *42*, 992.
[11] X. Wang, J. Zhang, Y. Yang, W. Dong, F. Wang, L. Wang, X. Li, *Exper. Therapeutic Med.* **2013**, *6*, 263.
[12] B. Yang, B. Li, C. Xu, S. Hu, M. Dai, J. Xia, P. Luo, X. Shi, Z. Zhao, X. Dong, Z. Fei, F. Fua, *NeuroImage: Clin.* **2019** *23*, 101909.
[13] R. M. Jha, P. M. Kochanek, J. M. Simard, *Neuropharmacology* **2019**, *145*, 230.
[14] D. K. Menon, C. Bryant, *Lancet Neurol.* **2019**, *18*, 28.
[15] M. Faul, L. Xu, M. M. Wald, V. Coronado, A. M. Dellinger, *Injury Prevention* **2010**, *16*, 1.
[16] Q. Wang, W. Fan, Y. Cai, Q. Wu, L. Mo, Z. Huang, H. Huang, *Amino Acids* **2016**, *48*, 2169.

 © 2021 The Authors. Advanced NanoBiomed Research published by Wiley-VCH GmbH

26999307, 2021, 11, Downloaded from https://advanced.onlinelibrary.wiley.com/doi/10.1002/anbr.202100001 by Koc University, Wiley Online Library on [05/09/2026]. See the Terms and Conditions (https://onlinelibrary.wiley.com/terms-and-conditions) on Wiley Online Library for rules of use; OA articles are governed by the applicable Creative Commons License

[17] V. C. Nikolian, S. E. Dekker, T. Bambakidis, G. A. Higgins, I. S. Dennahy, P. E. Georgoff, A. M. Williams, A. V. Andjelkovic, H. B. Alam, *Critical Care Med.* **2018**, *46*, 5.
[18] Centers for Disease Control and Prevention, *Report to congress on traumatic brain injury in the United States: Epidemiology and rehabilitation*, Centers for Disease Control and Prevention, Atlanta, GA **2015**.
[19] B. Tucker, J. Aston, M. Dines, E. Caraman, M. Yacyshyn, M. McCarthy, J. E. Olson, *J. Emerg. Med.* **2017**, *53*, 18.
[20] A. Colantonio, G. Gerber, M. Bayley, R. Deber, J. Yin, H. Kim, *J. Rehabilitation Med.* **2011**, *43*, 311.
[21] J. N. M. Schieveld, S. van Tuijl, T. Pikhard, *Critical Care Med.* **2013**, *41*, 1160.
[22] M. M. Tisdall, M. Smith, *Br. J. Anaesth.* **2006**, *97*, 18.
[23] H. Tumani, H.-P. Hartung, B. Hemmer, C. Teunissen, F. Deisenhammer, G. Giovannoni, U. K. Zettl, *Neurobiol. Dis.* **2009**, *35*, 117.
[24] A. M. Naidech, *Am. J. Respiratory Crit. Care Med.* **2011**, *184*, 998.
[25] H. Adrian, K. Mårten, N. Salla, V. Lasse, *eNeuro* **2016**, *3*, 1.
[26] J. A. Khoury, K. H. Noe, J. F. Drazkowski, J. I. Sirven, R. S. Zimmerman, *Epilepsia* **2011**, *52*, 123.
[27] M. L. Pearn, I. R. Niesman, J. Egawa, A. Sawada, A. Almenar-Queralt, S. B. Shah, J. L. Duckworth, B. P. Head, *Cell. Mol. Neurobiol.* **2017**, *37*, 571.
[28] H. Zetterberg, D. H. Smith, K. Blennow, *Nat. Rev. Neurol.* **2013**, *9*, 201.
[29] R. Allen, *J. Med. Eng. Technol.* **1986**, *10*, 299.
[30] A. M. Hudak, L. Peng, C. Marquez de la Plata, J. Thottakara, C. Moore, C. Harper, R. McColl, E. Babcock, R. Diaz-Arrastia, *Brain Injury* **2014**, *28*, 1602.
[31] J. A. Stokum, V. Gerzanich, J. M. Simard, *J. Cerebr. Blood Flow Metab.* **2016**, *36*, 513.
[32] E. A. Winkler, D. Minter, J. K. Yue, G. T. Manley, *Neurosurg. Clin. North Am.* **2016**, *27*, 473.
[33] S. Yeoh, E. D. Bell, K. L. Monson, *Ann. Biomed. Eng.* **2013**, *41*, 2206.
[34] M. Smith, *Anesthesiology* **2018**, *128*, 401.
[35] S.-M. Kim, S. H. Kim, D.-W. Seo, K.-W. Lee, *J. Korean Med. Sci.* **2013**, *28*, 1261.
[36] M. Oddo, F. Villa, G. Citerio, *Curr. Opin. Critical Care* **2012**, *18*, 111.
[37] P. Le Roux, D. K. Menon, G. Citerio, P. Vespa, M. K. Bader, G. M. Brophy, M. N. Diringer, N. Stocchetti, W. Videtta, R. Armonda, N. Badjatia, J. Böesel, R. Chesnut, S. Chou, J. Claassen, M. Czosnyka, M. De Georgia, A. Figaji, J. Fugate, R. Helbok, D. Horowitz, P. Hutchinson, M. Kumar, M. McNett, C. Miller, A. Naidech, M. Oddo, D. Olson, K. O'Phelan, J. J. Provencio, et al., *Neurocrit. Care* **2014**, *21*, 1.
[38] P. H. Raboel, J. Bartek, M. Andresen, B. M. Bellander, B. Romner, *Crit. Care Res. Pract.* **2012**, *2012*, 3.
[39] C. Heck, *Crit. Care Nurs. Clin. North Am.* **2016**, *28*, 77.
[40] X. Zhang, J. E. Medow, B. J. Iskandar, F. Wang, M. Shokoueinejad, J. Koueik, J. G. Webster, *Physiol. Measure.* **2018**, *39*, 058002.
[41] N. Carney, A. M. Totten, C. O'Reilly, J. S. Ullman, G. W. Hawryluk, M. J. Bell, S. L. Bratton, R. Chesnut, O. A. Harris, N. Kissoon, A. M. Rubiano, L. Shutter, R. C. Tasker, M. S. Vavilala, J. Wilberger, D. W. Wright, J. Ghajar, *Neurosurgery* **2017**, *80*, 6.
[42] S. K. Lee, J. P. S. Goh, *Proc. Singapore Healthc.* **2010**, *19*, 319.
[43] M. Swierczewska, G. Liu, S. Lee, X. Chen, *Chem. Soc. Rev.* **2012**, *41*, 2641.
[44] S. Dudal, D. Baltrukonis, R. Crisino, M. J. Goyal, A. Joyce, K. Österlund, J. Smeraglia, Y. Taniguchi, J. Yang, *AAPS J.* **2014**, *16*, 194.
[45] World Health Organization, *Screening Donated Blood for Transfusion-Transmissible Infections*, World Health Organization, Geneva **2010**.
[46] E. B. Aydın, M. K. Sezgintürk, *Anal. Biochem.* **2018**, *554*, 44.
[47] Y. Su, W. Fan, Z. Ma, X. Wen, W. Wang, Q. Wu, H. Huang, *Neuroscience* **2014**, *266*, 56.
[48] D. A. Armbruster, T. Pry, *Clin. Biochem. Rev.* **2008**, *29*, S49.
[49] P. Sharma, V. Semwal, B. D. Gupta, *Opt. Fiber Technol.* **2019**, *52*, 101962.
[50] M. Ben Ismail, E. Serna, G. Ruiz-Vega, T. García-Berrocoso, J. Montaner, M. Zourob, A. Othmane, E. Baldrich, *Anal. Chim. Acta* **2018**, *999*, 144.
[51] A. Ghosh, C. Elwell, M. Smith, *Anesthesia Analgesia* **2012**, *115*, 1373.
[52] S. H. Haddad, Y. M. Arabi, *Scand. J. Trauma Resuscit. Emer. Med.* **2012**, *20*, 1.
[53] R. Nangunoori, E. Maloney-Wilensky, M. Stiefel, S. Park, W. Andrew Kofke, J. M. Levine, W. Yang, P. D. Le Roux, *Neurocrit. Care* **2012**, *17*, 131.
[54] E. W. Lang, J. M. Mulvey, Y. Mudaliar, N. W. C. Dorsch, *Neurosurg. Rev.* **2007**, *30*, 99.
[55] S. B. Lewis, J. A. Myburgh, E. L. Thornton, P. L. Reilly, *Crit. Care Med.* **1996**, *24*, 1334.
[56] S. H. Friess, J. Ralston, S. A. Eucker, M. A. Helfaer, C. Smith, S. S. Margulies, *Neurosurgery* **2011**, *69*, 1139.
[57] N. Tasneem, E. A. Samaniego, C. Pieper, E. C. Leira, H. P. Adams, D. Hasan, S. Ortega-Gutierrez, *Crit. Care Res. Pract.* **2017**, *2017*. 6097265.
[58] L. Carteron, P. Bouzat, M. Oddo, *Front. Neurol.* **2017**, *8*, 1.
[59] J. Nortje, A. K. Gupta, *Br. J. Anaesth.* **2006**, *97*, 95.
[60] K. Fink, J. Fink, *Surg. Neurol. Int.* **2013**, *4*, 209.
[61] R. Naqi, M. Azeemuddin, *J. Pak. Med. Assoc.* **2013**, *63*, 399.
[62] C. Vanpeteghem, A. Moerman, S. De Hert, *J. Cardiothor. Vasc. Anesthesia* **2016**, *30*, 491.
[63] D. Joshi, J. O'Grady, A. Patel, D. Shawcross, S. Connor, N. Deasy, C. Willars, W. Bernal, J. Wendon, G. Auzinger, *Liver Int.* **2014**, *34*, 362.
[64] H. Utsunomiya, *Brain Dev.* **2011**, *33*, 235.
[65] D. Roh, S. Park, *Curr. Neurol. Neurosci. Rep.* **2016**, *16*. 56.
[66] B. Appavu, B. T. Burrows, S. Foldes, P. D. Adelson, *Front. Neurol.* **2019**, *10*, 1.
[67] D. Papadopoulos, A. Filippidis, G. Krommidas, G. Vretzakis, K. Paterakis, A. Komnos, K. N. Fountas, *Polish Neurol. Soc.* **2017**, *51*, 66.
[68] T. Westermaier, C. Stetter, E. Kunze, N. Willner, J. Holzmeier, J. Weiland, S. Koehler, C. Lotz, C. Kilgenstein, R.-I. Ernestus, N. Roewer, R. M. Muellenbach, *Neurocrit. Care* **2016**, *25*, 205.
[69] M. J. A. M. van Putten, J. Hofmeijer, *J. Clin. Neurophysiol.* **2016**, *33*, 203.
[70] G. Buzsáki, C. A. Anastassiou, C. Koch, *Nat. Rev. Neurosci.* **2012**, *13*, 407.
[71] C. R. Newey, A. Sarwal, S. Hantus, *Neurocrit. Care* **2013**, *18*, 261.
[72] Compumedics Neuroscan, 128-channels Quik-Cap Neo Net – SynAmps 2/RT and Neuvo, https://compumedicsneuroscan.com/product/128-channels-quik-cap-neo-net-synamps-2-rt-and-neuvo/.
[73] T. Partington, A. Farmery, *Anaesth. Intensive Care Med.* **2014**, *15*, 189.
[74] J. Ye, W. Zhang, M. Ye, *Med. Hypotheses* **2019**, *129*, 109257.
[75] O. Poch, I. Istiqomah, E. Quirico, P. Beck, B. Schmitt, P. Theulé, A. Faure, P. Hily-Blant, L. Bonal, A. Raponi, M. Ciarniello, B. Rousseau, S. Potin, O. Brissaud, L. Flandinet, G. Filacchione, A. Pommerol, N. Thomas, D. Kappel, V. Mennella, L. Moroz, V. Vinogradoff, G. Arnold, S. Erard, D. Bockelée-Morvan, C. Leyrat, F. Capaccioni, M. C. De Sanctis, A. Longobardo, F. Mancarella, et al., *Science* **2020**, *367*, 1.
[76] V. Wykes, R. Vindlacheruvu, *Surgery* **2015**, *33*, 355.
[77] G. Ormond, et al., Intracranial pressure (ICP) monitoring : information for families, **2019**.
[78] A. Sonig, F. Jumah, B. Raju, N. V. Patel, G. Gupta, A. Nanda, *World Neurosurg.* **2020**, *138*, 491.

© 2021 The Authors. Advanced NanoBiomed Research published by Wiley-VCH GmbH

26999307, 2021, 11, Downloaded from https://advanced.onlinelibrary.wiley.com/doi/10.1002/anbr.202100001 by Koc University, Wiley Online Library on [05/09/2026]. See the Terms and Conditions (https://onlinelibrary.wiley.com/terms-and-conditions) on Wiley Online Library for rules of use; OA articles are governed by the applicable Creative Commons License

[79] C. A. Gonzalez, J. A. Valencia, A. Mora, F. Gonzalez, B. Velasco, M. A. Porras, J. Salgado, S. M. Polo, N. Hevia-Montiel, S. Cordero, B. Rubinsky, M. Fehlings, *PLoS ONE* **2013**, *8*, e63223.
[80] D. W. McBride, J. I. Szu, C. Hale, M. S. Hsu, V. G. Rodgers, D. K. Binder, *J. Neurotrauma* **2014**, *31*, 1948.
[81] T. Reinecke, L. Hagemeier, H. Spehlbrink, S. Guenther, M. Klintschar, S. Zimmermann, *Sens. Actuators, B* **2014**, *204*, 763.
[82] T. Reinecke, L. Hagemeier, S. Ahrens, Y. Doroschenko, M. Klintschar, S. Zimmermann, *Sens. Actuators, B* **2015**, *220*, 522.
[83] Y. Jiang, M. Zhao, H. Wang, G. Li, *IOP Conf. Ser.: Earth Environ. Sci.* **2018**, *111*, 012027.
[84] D. Yang, S.-Y. Li, C.-M. Yeung, R. C. Chang, K.-F. So, D. Wong, A. C. Y. Lo, M. A. Deli, *PLoS ONE* **2012**, *7*, 33596.
[85] J. A. Stokum, V. Gerzanich, J. M. Simard, J. M. Simard, K. N. Sheth, W. T. Kimberly, Annual *Rev. Pharmacol. Toxicol.* **2020**, *60*, 291.
[86] C.-M. Cui, J.-L. Gao, Y. I. N. G. Cui, L.-Q. Sun, Y.-C. Wang, K.-J. Wang, R. A. N. Li, Y.-X. Tian, J.-Z. Cui, *Mol. Med. Rep.* **2015**, *12*, 2323.
[87] R. Kunze, A. Urrutia, A. Hoffmann, H. Liu, X. Helluy, M. Pham, S. Reischl, T. Korff, H. H. Marti, *Exp. Neurol.* **2015**, *266*, 99.
[88] M. Ke, X.-J. Zhang, Z.-H. Han, H.-Y. Yu, Y. Lin, W.-G. Zhang, F.-H. Sun, T.-J. Wang, *Carbohydrate Polymers* **2011**, *86*, 136.
[89] Y. Esquenazi, V. P. Lo, K. Lee, *J. Intens. Care Med.* **2017**, *32*, 15.
[90] M. R. Del Bigio, A. V. Shulyakov, Device to Reduce Brain Edema By Surface Dialysis and Cooling, https://lens.org/158-663-769-775-41X.
[91] A. I. Qureshi, J. I. Suarez, A. Bhardwaj, Malignant cerebral edema in patients with hypertensive intracerebral harmorrhage associated with sypertonic saline infusion, **1998**.
[92] Y. Zheng, E. Zheng, W. Hu, US 201161542314, **2011**.
[93] R. Wyeth, M. Levinson, US 201261588516, **2012**.
[94] MarketsandMarkets, Brain Monitoring Market – Global Forecast to 2025 | MarketsandMarkets, https://www.marketsandmarkets.com/Market-Reports/brain-monitoring-devices-market-909.html (accessed: September 2020).
[95] P. Rukskul, Analysis of different respiratory and blood gas parameters to optimize brain tissue oxygen tension (PtiO2) in patients with acute subarachnoid hemorrhage, **2015**.
[96] J. Chan, Online near-infrared spectroscopy brain-computer interfaces with real-time feedback, Doctoral Dissertation, **2011**.
[97] R. Helbok, M. Kofler, A. J. Schiefecker, M. Gaasch, V. Rass, B. Pfausler, R. Beer, E. Schmutzhard, *Front. Neurol.* **2017**, *8*, 491.
[98] The NHS, Electroencephalogram (EEG), https://www.nhs.uk/conditions/electroencephalogram/ (accessed: September 2020).
[99] B. Foreman, D. Cass, J. Forbes, L. B. Ngwenya, *J. Visual. Exp.* **2019**, *145*, 1.
[100] A. Abdalla Mohamed, W. Ahmed Ibrahim, T. Fayez Safan, *Egypt. J. Anaesthesia* **2011**, *27*, 273.
[101] M. Brasure, *Multidisciplinary Postacute Rehabilitation for Moderate to Severe Traumatic Brain Injury in Adults*, Agency for Healthcare Research and Quality, Rockville, MD **2012**.
[102] A. Gajofatto, S. Monaco, M. Fiorini, G. Zanusso, M. Vedovello, F. Rossi, M. Turatti, M. D. Benedetti, *Arch. Neurol.* **2010**, *67*, 724.
[103] N. Tanuma, R. Miyata, K. Nakajima, A. Okumura, M. Kubota, S.-i. Hamano, M. Hayashi, *Mediators Inflammation* **2014**, *2014*, 564091.
[104] H. Hegen, F. Deisenhammer, *LaboratoriumsMedizin* **2009**, *33*, 321.
[105] Jérôme. Badaut, A. M. Fukuda, A. Jullienne, K. G. Petry, *Biochim. Biophys. Acta* **2014**, *1840*, 1554.
[106] P. Shahim, J.-E. Månsson, N. Darin, H. Zetterberg, N. Mattsson, *Eur. J. Paediatr. Neurol.* **2013**, *17*, 7.
[107] Y. T. Cheung, R. B. Khan, W. Liu, T. M. Brinkman, M. N. Edelmann, W. E. Reddick, D. Pei, A. Panoskaltsis-Mortari, D. Srivastava, C. Cheng, L. L. Robison, M. M. Hudson, C.-H. Pui, K. R. Krull, *JAMA Oncol.* **2018**, *4*, 1.
[108] N. Mattsson, U. Andreasson, S. Persson, H. Arai, S. D. Batish, S. Bernardini, L. Bocchio-Chiavetto, M. A. Blankenstein, M. C. Carrillo, S. Chalbot, E. Coart, D. Chiasserini, N. Cutler, G. Dahlfors, S. Duller, A. M. Fagan, O. Forlenza, G. B. Frisoni, D. Galasko, D. Galimberti, H. Hampel, A. Handberg, M. T. Heneka, A. Z. Herskovits, S.-K. Herukka, D. M. Holtzman, C. Humpel, B. T. Hyman, K. Iqbal, M. Jucker, et al., *Alzheimer's Dementia* **2011**, *7*, 386.
[109] G. R. Criscuolo, *Yale J. Biol. Med.* **1993**, *66*, 277.
[110] N. Shadjou, S. Alizadeh, M. Hasanzadeh, *J. Mol. Recogn.* **2018**, *31*, 1.
[111] S. Scarano, E. Dausse, F. Crispo, J.-J. Toulmé, M. Minunni, *Anal. Chim. Acta* **2015**, *897*, 1.
[112] W. Zhang, Z. He, L. Yi, S. Mao, H. Li, J.-M. Lin, *Biosens. Bioelectron.* **2018**, *102*, 652.
[113] A. Bosnjakovic, M. K. Mishra, H. J. Han, R. Romero, R. M. Kannan, *Anal. Chim. Acta* **2012**, *720*, 118.
[114] S. Ghosh, D. Datta, S. Chaudhry, M. Dutta, M. A. Stroscio, *IEEE Trans. Nanobiosci* **2018**, *17*, 417.
[115] E. Sánchez-Tirado, C. Salvo, A. González-Cortés, P. Yáñez-Sedeño, F. Langa, J. M. Pingarrón, *Anal. Chim. Acta* **2017**, *959*, 66.
[116] A. S. Ghrera, *Analy. Chim. Acta* **2019**, *1056*, 26.
[117] P. Seshadri, K. Manoli, N. Schneiderhan-Marra, U. Anthes, P. Wierzchowiec, K. Bonrad, C. Di Franco, L. Torsi, *Biosens. Bioelectron.* **2018**, *104*, 113.
[118] A. M. H. Young, M. R. Guilfoyle, J. Donnelly, P. Smielewski, S. Agarwal, M. Czosnyka, P. J. Hutchinson, *Pediatr. Res.* **2018**, *83*, 41.
[119] A. Bhardwaj, J. A. Ulatowski, *Curr. Treat. Options Neurol.* **1999**, *1*, 179.
[120] K. P. Budohoski, *Intracranial Compartment and Intracranial Pressure. Gupta Gelb's Essentials Neuroanesthesia Neurointensive Care*, **2018**, pp. 31–38.



Karthikeya Deshmukh is a Ph.D. student in the Department of Chemical Engineering and Biotechnology at the University of Cambridge. His research focuses on improving the cleaning performance of cleaning-in-place systems used in the manufacturing industry by optimizing fluid properties. He completed his master's degree in Advanced Chemical and Biotechnology from Imperial College London and an undergraduate degree in Chemical Engineering from Loughborough University. His master's thesis focused on writing a literature review on the current and emerging technologies for the effective diagnosis and treatment of cerebral edema.

© 2021 The Authors. Advanced NanoBiomed Research published by Wiley-VCH GmbH

26999307, 2021, 11, Downloaded from https://advanced.onlinelibrary.wiley.com/doi/10.1002/anbr.202100001 by Koc University, Wiley Online Library on [05/09/2026]. See the Terms and Conditions (https://onlinelibrary.wiley.com/terms-and-conditions) on Wiley Online Library for rules of use; OA articles are governed by the applicable Creative Commons License



Savas Tasoglu received his Ph.D. degree in 2011 from UC Berkeley and held a postdoctoral appointment at Harvard Medical School. His research interests are at the interfaces of complex microfluidics, transport phenomena, and biomaterials with applications in biomedicine and biotechnology. He has received several awards, including a Marie Curie Fellowship, American Heart Association Scientist Development Award, NIH K99/R00 Pathway to Independence Award (declined), Alexander von Humboldt Fellowship for Experienced Researchers, and the Wolff New Venture Competition Award.



Ali K. Yetisen researches optical biosensors, wearable devices, implantable chips, and personalized medicine. He was previously a Tosteson postdoctoral fellow at Harvard University. He holds a Ph.D. degree in chemical engineering and biotechnology from the University of Cambridge. He has been awarded several international prizes, including the IChemE Nicklin Medal, Birmingham Fellowship, and Alexander von Humboldt Fellowship. He is a Fellow of the Royal Society of Chemistry.

© 2021 The Authors. Advanced NanoBiomed Research published by Wiley-VCH GmbH

26999307, 2021, 11, Downloaded from https://advanced.onlinelibrary.wiley.com/doi/10.1002/anbr.202100001 by Koc University, Wiley Online Library on [05/09/2026]. See the Terms and Conditions (https://onlinelibrary.wiley.com/terms-and-conditions) on Wiley Online Library for rules of use; OA articles are governed by the applicable Creative Commons License